"FORMULATION AND CHARACTERIZATION OF PECTIN-NANOPARTICLES LOADED IN-SITU INTRANASAL GEL OF VENLAFAXINE HYDROCHLORIDE "

A Thesis Submitted to

NIRMA UNIVERSITY

In Partial Fulfillment for the Award of the Degree of

MASTER OF PHARMACY
IN
PHARMACEUTICAL TECHNOLOGY & BIOPHARMACEUTICS

BY

PARTH RAMESHCHANDRA DAVE (13MPH116), B. PHARM.

Under the guidance of

Mr. VENUGOPALA C.J
Group Leader, Formulation Research Department, Aurobindo Pharma Ltd., Hyderabad.

Dr. MAYUR M. PATEL
Associate Professor, Department of Pharmaceutics, Institute of Pharmacy, Nirma University, Ahmedabad.

Department of Pharmaceutics
Institute of Pharmacy
Nirma University
Ahmedabad-382481

INSTITUTE OF PHARMACY, NIRMA UNIVERSITY

DECLARATION

I hereby declare that the dissertation entitled "Formulation Development and Optimizaation of Capsule Comprising Immediate and Extended Release System" submitted by Mr. Parth Rameshchandra Dave with Regn. No. (13MPH116), is based on the original work carried out by me under the guidance of Mr. Venugopala C.J, Group Leader, Aurobindo Pharma LTD, and Dr. Mayur M. Patel, Associate Professor, Department of Pharmaceutics, Institute of Pharmacy, Nirma University. I also affirm that this work is original and has not been submitted in part or full for any other degree or diploma to this or any other university or institution.

Mr. PARTH RAMESHCHANDRA DAVE (13MPH116)
Department of Pharmaceutics,
Institute of Pharmacy,
Nirma University,
Sarkhej - Gandhinagar Highway,
Ahmedabad-382481,
Gujarat, India

Date: 24th May, 2015

CERTIFICATE

This is to certify that the dissertation work entitled "Formulation and Characterization of Pectin-Nanoparticles loaded In-Situ Intranasal Gel of Venlafaxine Hydrochloride" submitted by Mr. Parth Manilal Patel with Regn. No. (13MPH117) in partial fulfillment for the award of Master of Pharmacy in "Pharmaceutical Technology and Biopharmaceutics" is a bonafide research work carried out by the candidate at the Accuprec Research Lab. Pvt. Ltd., Ahmedabad under our guidance. This work is original and has not been submitted in part or full for any other degree or diploma to this or any other university or institution.

Industrial Guide

Dr. Rina M. Gokani
M. Pharm.,Ph.D.,
Director
Accuprec Research Lab
Pvt.Ltd.
Ahmedabad

Academic Guide:

Dr. Mayur M. Patel
M. Pharm., Ph.D.,
Associate Professor,
Department of Pharmaceutics,
Institute of Pharmacy,
Nirma University

Prof. Tejal Mehta
M. Pharm., Ph.D.
Professor & Head,
Department of Pharmaceutics,
Institute of Pharmacy,
Nirma University

Prof. Manjunath Ghate
M. Pharm., Ph.D.
Director
Institute of Pharmacy,
Nirma University

Date : 23rd May, 2015

Acknowledgements

It gives me immense pleasure today when I take an opportunity to acknowledge all those personalities who contributed directly or indirectly to my project. This research would not have been possible without the whole hearted encouragement, guidance, support and cooperation of my beloved family, teachers, friends, well wishers and relatives. Probably I would never have achieved this without their support and blessings. With profound appreciation, I acknowledge to one and all I take this opportunity to proudly place on record my profound sense of gratitude to ***Dr.Manjunath Ghate****, director of Institute of Pharmacy, Nirma University, Ahmedabad for his valuable guidance, encouragement and continued support throughout the course of this work.*

I am equally thankful to ***Dr. Tejal A. Mehta*** *Head, Dept. of Pharmaceutics, Institute of Pharmacy, Nirma University for her unending encouragement, friendly nature, timely suggestions and total understanding.*

With profound pleasure, I express my deepest gratitude to my esteemed guide, ***Dr. Mayur Patel,*** *Associate Professor, Department of Pharmaceutics and Pharmaceutical Technology, Institute of Pharmacy, Nirma University for his erudite guidance, timely suggestions, continuous encouragement and critical remarks for the entire span of my work. I look him as my ideal and treasure, the relationship with him as a student and a human being now and forever in future.*

I express my warmest gratitude to my guide ***Mr. Venugopala C.J****, Group Leader, RC-1, Aurobindo Pharma Ltd. for his valuable guidance, keen interest, perennial inspiration and everlasting encouragement. It is with affection and reverence that I acknowledge my indebtness to him for outstanding dedication, often far beyond the call of duty.*

INSTITUTE OF PHARMACY, NIRMA UNIVERSITY

I would like to thank Mr. Satyabrata Barik, Mr. Krishnakumar Chegunda, Mr. Srinivas Balla, Mr. Shubhakanta Dhal, Mr.Diptiranjan Parida, and all Aurobindo family for their selfless support, co-operation and valuable suggestions.

I am extremely grateful to Dr. Dhaivat Parikh, Dr. Shital Bariya, Dr. Renuka Mishra, Dr. Jigar N shah, Dept. of Pharmaceutics, Institute of Pharmacy, Nirma University for their continuous encouragement and everlasting support throughout the course of this dissertation work.

Friends are the treasures that one can count on in difficult times. This thesis is the result of constant encouragement and help of my friends, especially, Pratik Chauhan, Mayur Prajapati, Maulik Chaudhari, Ketul Prajapati, Yash Raj, Apoorva Patel, Harnish Patel, Raviteja Nalla, Jigar Patel, Jatin Patel, and Jitendra Patel.

I would also like to acknowledge my colleagues, ***Monil Soni, Parth Patel, Shreyash Shah, Darshan Goswami, kasim Shaikh, Jahid Tanwar, Ronak Vashi, Jitendra Sharma, Ankit Gotecha, Khushali Modi, Khushbu Trivedi, Pankti Vasani, Pooja Patel, Bhavna Singh, Anuradha Vanzara, Mimansha Jhaveri,*** *for their help throughout my work.*

I would like to thank Ph.D. student ***Nimit Chokshi*** *for his support.*

How can I forget sweet moments spent with my hostel friends Maulik Ranpariya, Smit Patel, Ronak Vashi, Khushbu Trivedi, Rahul Mahale, Suja Varghese, and Pratap Dakua. I would like to thank them to help me complete my project work.

I sincerely thanks to Mrs. P. Lalitha and Rajubhai for library facilities and constant encouragement during my work.

INSTITUTE OF PHARMACY, NIRMA UNIVERSITY

I also wish to acknowledge ***Shaileshbhai, Satejbhai, Shreyasbhai, Ravindrabhai, Mukeshbhai, Rameshbhai, Kiranbhai, Vikrambhai, Sanjaybhai*** *and* ***Devrajbhai*** *for providing me the materials required in my work.*

I also wish to acknowledge ***Lalabhai, Ranjitbhai, Harish, Panditbhai, Rameshbhai, Hasmukhbhai, Lekha, Pooja, Foram, Madhuri, Punit, Darshit, Praful, Jaswant, Pratap, Aakash, Ashesh, Viralbhai, Sweta, Avish*** *for their constant help.*

Last but not the least, I am indebted infinitely to love, care, patience and trust being showered on me by my family- ***My Father, My Mother*** *and* ***my Sister****, With their consistent prayers, affectionate blessings, selfless care and endless confidence in me. I would have never come to this stage of writing this acknowledgement.*

Parth R. Dave

Date: 25th May, 2015
Place: Institute of Pharmacy,
Nirma University,
Ahmedabad.

INDEX

LIST OF TABLES

LIST OF FIGURES

CSF	Cerebrospinal fluid
CNS	Central Nervous System
VLF	Venlafaxine
TJ	Tight junctions
MW	Molecular weight
IN	Intranasal
OSN	Olfactory sensory neurons
OEC	Olfactory ensheathing cells
HBC	Horizontal basal cells
GBC	Globose basal cells
ICA	Internal carotid artery
HRP	HorseraDish Peroxidase
WGAHRP	Wheat germ agglutinin-horseradish peroxidase
GAD	Generalized anxiety disorder
ODV	O-desmethyl venlafaxine
SNRI	Serotonin Norepinephrine reuptake inhibitor
SNDRI	Serotonin-Norepinephrine-Dopamine reuptake inhibitor
ECT	Electroconvulsive therapy
GFR	Glomerular Filtration Rate
MAOI	Monoamine oxidase inhibitor
USFDA	US Food and Drug Administration body
PCP	Positive phencyclidine
GalA	D-galacturonic acid
Rha	Rhamnose
HM-pectin	High methoxy pectin
LM-pectin	Low methoxy pectin
$MgCl_2$	Magnesium Chloride
$CaCl_2$	Calcium Chloride
$ZnCl_2$	Zinc Chloride
JP	Japanese Pharmacopoiea
EP	Euroean Pharmacopoiea
USP	United States Pharmacopoiea
NF	National Formulary
HEMA	Hydroxyethyl methacryate
HPMA	N-(2-Hydroxypropyl) methacrylate
NVP	N-Vinyl-2-pyrrolidone
NIPAMM	N-Isopropylacrylamide
VAc	Vinyl acetate
AA	Acryolic acid
GRAS	Generally Recognized as safe
ADME	Absorption, Distribution, Metabolism and Elimination
TPP	Tripolyphosphate anions
OZ	Olanzapine
MRI	Magnetic Resonance image
UEA I	Ulex europeus agglutinin I
PEG-PLA	Poly(ethylene glycol)–poly(lactic-co-glycolic

	acid
UCN	Urocortin peptide
TH	Tyrosine hydroxylase
SME	Sumatriptan microemulsions
SSME	Sumatriptan succinate microemulsions
DTE	Drug targeting efficiency
IV	Intravenous
DTP	Direct drug transport
AUC	Area under the curve
HPMC K4M	Hydroxyl Propyl Methyl Cellulose K4M
TDM	n-tridecyl-d-maltoside
CRV	Carvedilol
ZDV	Zidovudine
THA	Tacrine
FTIR	Fourier Transform Infrared Spectroscopy

ABSTRACT

Formulation and Characterization of Pectin-Nanoparticles loaded In-Situ Intranasal Gel of Venlafaxine Hydrochloride

Patel Parth[1], Patel Mayur[1], Gokani Rina[2]

1. Institute of Pharmacy, Nirma University, Ahmedabad - 382481.

2. Accuprec Research Lab PVT. LTD.- Gandhinagar - 380061

Email : 13mph117@nirmauni.ac.in

The purpose of the present investigation was to prepare venlafaxine (VLF) loaded pectin nanoparticles (NPs) incorporated into thermosensitive insitu gelling solution that will undergo gelation at nasal temperature, to enhance the uptake of VLF to brain via intranasal (i.n.) delivery. VLF loaded pectin NPs were prepared and characterized for particle size, zeta potential, encapsulation efficiency and in vitro drug release. The low bioavailability and systemic side effects exhibited by conventional oral dosage forms of venlafaxine hydrochloride due to high hepatic first pass metabolism of the drug may be overcome by the use of in situ gel-forming systems that are instilled as solution into the nasal cavity that will result in brain targeting via olfactory region. Further formulation of venlafaxine hydrochloride into nanoparticles will result in sustained drug delivery for a longer duration that is best suitable for anti depressive therapy. Nanoparticles were prepared using ionic gelation technique in which pectin was used as polymeric phase and $MgCl_2$, $CaCl_2$, $ZnCl_2$ as divalent cation and different pH conditions of pectin solution (pH 2.0, pH 4.0, pH 6.0) were used for the formulation of nanoparticles. Results of preliminary batches revealed that nanoparticles prepared using $MgCl_2$ as a cation and pH of pectin solution at 4.0 was found to possess lowest particle size, optimum zeta potential, optimum % entrapment efficiency and complete drug release at 24 hours. For the systematic optimization of the prepared nanoparticles a 3^2 full factorial design was used with Pectin:$MgCl_2$ concentration ratio and pH of the

pectin solution as independent variables and particle size, zeta potential, % entrapment efficiency and % drug release at 24 hours as dependent variables. Results of different batches prepared using factorial design revealed that nanoparticles prepared using 0.5% pectin solution, 0.5 % $MgCl_2$ and pH 4.0 of pectin solution had lowest particle size (170.8 nm), optimum zeta potential (-28.9 mV), optimum % entrapment efficiency (76.2%) and complete drug release at 24 hours (90.36%). The prepared nanoparticles were incorporated into thermosensitive insitu gelling solution (25% poloxamer 407 and 0.5% HPMC K4M) that undergoes gelation within < 40 seconds at 31^{o}C. The results demonstrated that the nanoparticulate insitu gelling suspension can be used for nasal administration of venlafaxine hydrochloride to enhance the CNS targetting, bioavailability and patient compliance.

1. AIM of Present Investigation

Currently venlafaxine is available as oral dosage forms like tablets and capsules. Conventional drug delivery methods fail to deliver a number of therapeutic agents to the brain efficiently as blood brain barrier (BBB) and blood–cerebrospinal fluid (CSF) barrier restrict the transport of drugs from systemic circulation into the central nervous system (CNS). Oral dosage forms have several disadvantages like low bioavailability and systemic side effect. A number of invasive strategies like intraparenchymal, intraventricular, intrathecal delivery (BBB disruption) and non-invasive techniques like chemical modifications, prodrug approach and conjugation of a drug with antibodies or ligands have been used to increase the CNS targeting of drugs but all these techniques are invasive. So it is necessary to develop sustained release dosage form of venlafaxine that will result in drug release for a longer period of time. Sustained release (SR) drug delivery systems are developed to modulate the release of drug, in order to achieve specific clinical objectives that cannot be attained with conventional dosage forms. Possible therapeutic benefits of a properly designed SR dosage form include low cost, simple processing, improved efficacy, reduced adverse events, flexibility in terms of the range of release profiles attainable, increased convenience and patient compliance. Incorporation of drug in the matrix of hydrophilic and hydrophobic polymers have been successfully employed in the development of sustained release delivery systems to provide the desired release profile.

Venlafaxine (VLF) is amongst the first line drugs used in the treatment of depression. It inhibits central serotonin and norepinephrine neuronal reuptake increasing the diminished levels of neurotransmitters like serotonin and norepinephrine in the synaptic cleft between neurons in the brain. Venlafaxine is commercially available as immediate and controlled release tablets and capsules. VLF is one of the most widely used antidepressants but oral therapy has a number of drawbacks, such as slow onset of action, side effects like tachycardia, increased blood pressure, fatigue, headache, dizziness, sexual dysfunction, dry mouth and low bioavailability (40–45%). Additionally, VLF has an elimination half-life of 4–5 h and therefore needs frequent administration to maintain a blood level for effective therapeutic concentration. Efficacy of VLF relies upon its continued presence at the site of action over a prolonged period of time. However the saw-tooth pattern of plasma drug

concentrations following oral drug administration often causes adverse events at maxima and loss of therapeutic effect at minima, which leads to intolerability. This fact provides a strong rationale for designing more effective intranasal dosage forms capable of directly transporting the drug to the brain to maintain constant antidepressive effect and reduce side effects of conventional dosage forms. Insitu gel is in the form of solution at physical condition that gets converted into gel at physiological temperature.

Hence the aim of present investigation is to develop venlafaxine hydrochloride loaded pectin nanoparticles to be incorporated into insitu gelling poloxamer solution that will deliver drug to CNS via intranasal route for a longer period of time.

2. Introduction [1-4]

2.1 Introduction to intranasal drug delivery:

The blood–brain barrier (BBB) is located at the level of the cerebral microvasculature and is critical for maintaining central nervous system (CNS) homeostasis. Although the BBB restricts the entry of potentially neurotoxic substances into the brain, it also presents a major obstacle to the delivery of drugs into the CNS for disease treatment. The BBB exhibits a low rate of pinocytosis and possesses tight junctions (TJ) which form a seal between opposing endothelial membranes. The presence of TJ at the BBB creates a high transendothelial electrical resistance of 1500–2000 $\Omega \cdot cm^2$ compared to 3–30 $\Omega \cdot cm^2$ across most peripheral microvessels. This high resistance is associated with very low permeability, i.e. the BBB greatly restricts paracellular diffusion of solutes from the blood into the brain. Typically, only small, lipophilic molecules appreciably cross the normal, healthy BBB via transcellular passive diffusion, although some limited transport of certain peptides and peptide analogs has been reported. Essential nutrients such as glucose or iron gain entry into the CNS through specific transporters such as the glucose transporter 1 or receptors such as the transferrin receptor. Receptors and transporters for gastrointestinal hormones involved in regulating metabolism are expressed at the BBB in order to convey information between the CNS and periphery. In addition to its low paracellular permeability and low rate of pinocytosis, the BBB also expresses a high number of drug transporters (e.g. P-glycoprotein) which further restrict brain entry of many endogenous and exogenous substances that would otherwise be predicted to cross the BBB based on molecular weight (MW) and lipophilicity considerations. Although there are many examples of small MW drugs which cross the BBB, nearly all large MW substances are severely restricted from crossing the BBB under normal conditions; indeed, the only examples of large MW drugs approved for clinical use in treating a neurological illness are those that act via peripheral mechanisms (e.g. type I interferons for treating multiple sclerosis). However, it will likely be necessary to implement drug delivery strategies that overcome the formidable obstacles presented by the various barriers of the CNS (the BBB and blood–cerebrospinal fluid (CSF) barriers) for these studies to ultimately be translated to the clinic.

Intraparenchymal, intracerebroventricular and intrathecal injections/infusions are capable of delivering therapeutics directly to the CNS, but these routes of administration are invasive and likely not practical for drugs which need to be given chronically. The intranasal (IN) route of administration provides a non-invasive method of bypassing the BBB to potentially deliver biologics such as peptides, proteins, oligonucleotides, viral vectors and even stem cells to the CNS. The intranasal route has long been associated with a number of advantages, e.g. rapid onset of effects using noninjectable administration methods and a growing record with approved formulations (e.g. nasal spray of the 3.5 kDa polypeptide hormone calcitonin has been used for many years to treat postmenopausal osteoporosis); the major disadvantage of the route, aside from the challenge of reproducibility, is that limited absorption across the nasal epithelium has restricted its application to particularly potent substances, although this can be overcomed by use of permeation enhancers in some cases. Delivery of biologics and a variety of other substances from the nasal passages to the brain has now been documented in numerous animal and clinical studies.

2.1.1Advantages and disadvantages of intranasal drug delivery:

A) Advantages

- Non-invasive/reduced infection risk from application/low risk of disease transmission.
- Ease of self-administration/dose adjustment.
- Large surface area for absorption (human~160 cm^2).
- Rapid absorption/fast onset of action.
- Avoid hepatic first-pass elimination.
- Possible direct pathways to the CNS bypassing the blood–brain barrier.
- Rich, vascular submucosa and lymphatic system.

B) Disadvantages

- Limited to potent drugs/small volumes (25–200 μl).
- Active mucociliary clearance.

- Enzymatic degradation by nasal cytochrome P450/peptidases/proteases (pseudo first-pass effect).
- Low permeability for hydrophilic drugs without absorption enhancers necessitates large doses.
- Low pH of nasal epithelium.
- Interindividual variability.

2.1.2 Nasal anatomy:

2.1.2.1 General considerations:

The nasal cavity extends from the nostrils (nares) to the nasopharynx and is divided longitudinally by the nasal septum. The human nasal cavity only extends approximately 12–14 cm in length yet has a large absorptive surface area of ~160 cm^2 due to three bony structures called turbinates or conchae (inferior, middle and superior) which also aid in filtering, humidifying and warming inspired air. The architecture of the rat nasal passage is generally more complex than that of the primates, with a significantly higher surface area-to-volume ratio.

Inspiratory airflow route close to floor of nasal passage; vortex in vestibule upward and laterally respiratory mucosal cilia) is directed mostly anteriorly in rats while in primates nasal secretions are mostly transported posteriorly toward the nasopharynx. Macrosmatic species such as the rat have a significantly higher percentage of nasal epithelium devoted to olfaction (the sense of smell) compared to microsmotic species such as humans and monkeys. Nevertheless, studies in rats are critically important and have been used to establish much of about the pathways and mechanisms underlying nasal delivery to both the

systemic circulation and the CNS simply because it is far less practical to conduct certain types of research in primate species.

There are four types of epithelia in the nasal cavity: squamous, respiratory, transitional and olfactory. The nasal vestibule, extending from just inside the nares to the anterior portion of the inferior turbinates, is lined with stratified squamous epithelium which contains coarse hairs in addition to sebaceous and sweat glands. The transitional epithelium is a non-ciliated cuboidal or columnar epithelium located between the

squamous and respiratory epithelia and the respiratory and olfactory epithelia. Intranasal drug delivery system mainly focus on the olfactory and respiratory epithelia because they represent the most likely sites of absorption for drugs administered by this route.

2.1.2.2 Olfactory region:

The olfactory region comprises 10% of the surface area of the nasal epithelium. It consists of a pseudo-stratified columnar epithelium located on the most superior aspect of the nasal cavity that is responsible for mediating the sense of smell. Olfactory sensory neurons (OSN) have several unique attributes: they are the only first order neurons possessing cell bodies located in a distal epithelium and the tips of their dendritic processes, which end as enlarged knobs with several non-motile cilia, extend far into the overlying mucus layer that is directly exposed to the external environment (Fig. 2.1).

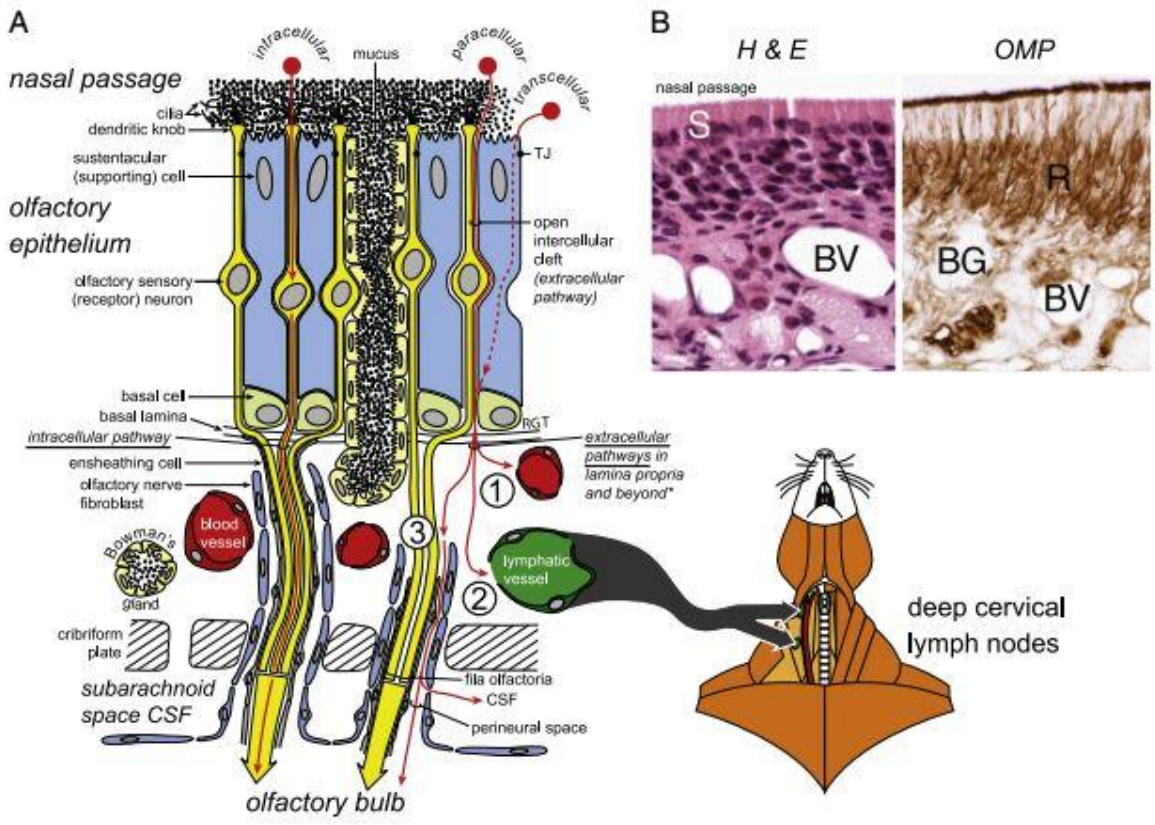

Fig. 2.1. General organization of the olfactory region.[2]

(A) The olfactory mucosa includes the olfactory epithelium and its underlying lamina propria. Axonal processes of olfactory sensory neurons converge into bundles (fila olfactoria), surrounded by ensheathing cells and fibroblasts, before projecting to the olfactory bulb. Potential pathways for drug delivery across the olfactory epithelium following intranasal administration are shown in red. Some substances may be transported by an intracellular pathway from the olfactory epithelium to the olfactory bulb within olfactory sensory neurons following adsorptive receptor-mediated or non-specific fluid phase endocytosis. Other substances may cross the olfactory epithelial barrier by paracellular or transcellular transport to reach the lamina propria, where a number of different extracellular pathways for distribution are possible, as indicated:
(1) absorption into olfactory blood vessels and entry into the general circulation;
(2) absorption into olfactory lymphatic vessels draining to the deep cervical lymph nodes of the neck;
(3) extracellular diffusion or convection in compartments associated with olfactory nerve bundles and entry into the cranial compartment.

Transport within the perineural space bounded by olfactory nerve fibroblasts is indicated but other possibilities exist, e.g. transport within the fila olfactoria compartment contained by ensheathing cells, transport within the perivascular spaces of blood vessels traversing the cribriform plate with olfactory nerves or transport within lymphatics traversing the cribriform plate with olfactory nerves. Possible pathways for distribution of substances from the perineural space into the olfactory subarachnoid space cerebrospinal fluid (CSF) or into the olfactory bulb are shown.

The OSN are bipolar cells possessing odorant responsive receptors in the plasma membrane of the olfactory cilia; easy access of odorants to OSN receptors in the mucus lining the olfactory epithelium is essential to the process of olfaction. The unmyelinated axons of OSN extend through the epithelial basal lamina and converge with axons from other OSN to form nerve bundles called fila olfactoria. Interlocking olfactory ensheathing cells (OEC) enclose the fila olfactoria in continuous channels from their origin to the olfactory bulb. The olfactory ensheathing cells are further enclosed by multicellular sheets of olfactory nerve fibroblasts to form a perineural-like sheath around the fila olfactoria. The ensheathed fila olfactoria comprise the olfactory nerve and travel through the cribriform plate of the ethmoid bone into the brain where

they terminate on dendrites of the mitral, periglomerular, and tufted cells in glomeruli of the olfactory bulb. Olfactory information is then sent through axons of the mitral and tufted cells to a number of areas including the anterior olfactory nucleus, olfactory tubercle, piriform cortex, amygdala and entorhinal cortex. Several other types of cells reside in the olfactory epithelium in addition to OSN. Sustentacular cells extend from the apical region of the epithelium to the basal lamina and act as supporting cells. They possess long, irregular microvilli which intermingle with the cilia of the OSN. Cells of the Bowman's gland form tubular-type ducts which originate in the lamina propria and traverse the basal lamina to produce and secrete a serous fluid which acts as a solvent for odor molecules.

There are also horizontal basal cells (HBC) and globose basal cells (GBC). The HBC are located along the basal lamina and act as multipotent progenitors to GBC, sustentacular cells and cells of the Bowman's gland and duct. The GBC are located slightly higher than the HBC in the olfactory epithelium and act as neural progenitors, providing a source for continual OSN replacement. Small populations of cells lined with numerous microvilli also exist in the olfactory epithelium. These cells are referred to as microvillus cells and have an unknown function. Blood vessels, inflammatory cells and lymphatic vessels which drain into the deep cervical lymph nodes in the neck are also present in the submucosa (lamina propria) of the olfactory region.

2.1.2.3 Respiratory region:

The nasal respiratory epithelium lines approximately 50% of the nasal cavity in rats and 80–90% in humans. It is a pseudostratified columnar secretory epithelium (Fig. 2.2) which warms and humidifies inspired air in addition to removing particulates, microorganisms and allergens.

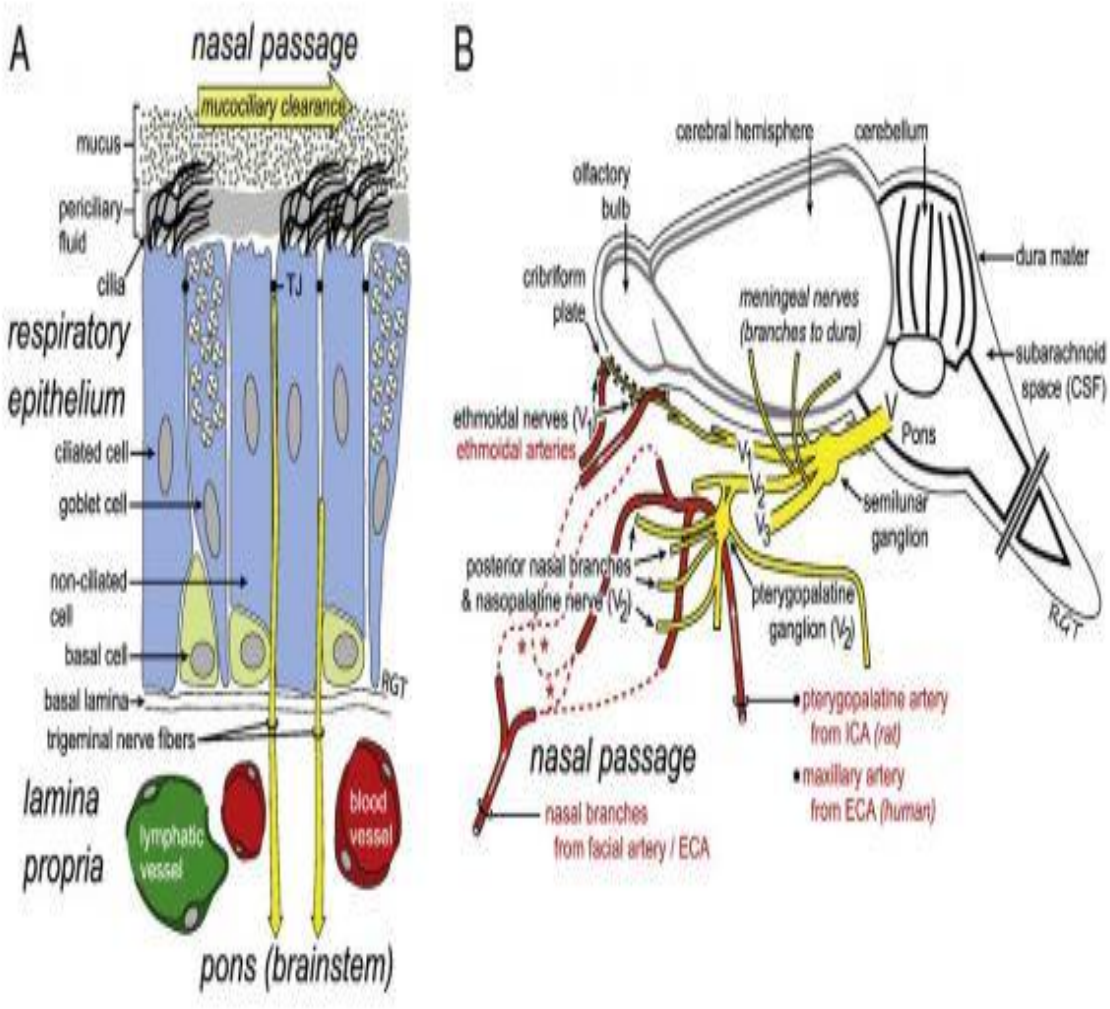

Fig. 2.2 General organization, trigeminal innervation and vasculature of the nasal respiratory region.[2]

(A) The respiratory mucosa includes the respiratory epithelium and its underlying lamina propria. Fibers of the trigeminal nerve, important for conveying chemosensory, touch and temperature information are found throughout the nasal epithelium where their free nerve endings extend nearly to the epithelial surface, just beneath tight junctions (TJ).

(B) Central projections of the trigeminal nerve shown together with the vasculature of the nasal passage. The cell bodies of the trigeminal nerve fibers are located in the semilunar ganglion; their axons project into the brainstem at the level of the pons where they ultimately synapse with neurons in brainstem areas such as the principal sensory and spinal trigeminal nuclei. Of the three main trigeminal nerve divisions (V1, the ophthalmic nerve; V2, the maxillary nerve; and V3, the mandibular nerve), only V1 and V2 send branches to the nasal epithelium.

Blood supply to the nasal passages is provided by ethmoidal branches of the ophthalmic artery, sphenopalatine branches of either the external carotid artery (ECA)/maxillary artery (in humans) or the internal carotid artery (ICA)/pterygopalatine artery (in rats), and nasal branches from the ECA/facial artery numerous anastomoses (*) connect these branches within the nasal passages.

The human respiratory epithelium is comprised of goblet cells, ciliated cells, intermediate cells and basal cells. Serous glands, seromucous glands and intraepithelial glands are also associated with the nasal respiratory epithelium. The seromucous glands are responsible for producing most nasal secretions while the goblet cells also secrete mucus. The primary role of the ciliated cells is to use their motile cilia, immersed in periciliary fluid to propel mucus towards the nasopharynx where it is either swallowed or expectorated. Basal cells function as progenitors to the other cell types in the nasal respiratory epithelium.

The nasal respiratory epithelium is innervated by branches of the trigeminal nerve; fibers from trigeminal ganglion cells ramify extensively within the nasal mucosa with many extending almost completely through the epithelium (both respiratory and olfactory) so that their free nerve endings lie very near the epithelial surface (stopping at the TJ level). The trigeminal nerve, or the fifth (V) cranial nerve is the largest of the twelve cranial nerves and its distribution and nasal passage innervations are well understood (Fig. 2.2 B). The trigeminal nerve exits the pons laterally and consists of a very large sensory root and a small motor root. It is therefore referred to as a mixed nerve, carrying motor fibers to the muscles of mastication and transmitting sensory information from the face, scalp, mouth and nasal passages. The trigeminal nerve runs underneath the dura as it courses rostrally. The three major branches of the trigeminal nerve include the ophthalmic nerve (V1), the maxillary nerve (V2) and the mandibular nerve (V3); the trigeminal nerve is mostly composed of somatic afferent fibers, i.e. sensory information is being conveyed into the brain from the nasal passages and other innervated areas. V1 and V2 are sensory nerves that also carry autonomic fibers. V3 contains the mixed portion of the trigeminal nerve, as it is joined by the trigeminal motor root which merges with V3 after passing underneath the semilunar (trigeminal) ganglion. In humans, V1 enters the cranial compartment through the superior orbital fissure, V2 enters the cranial compartment through the foramen rotundum, and V3

enters the cranial compartment through the foramen ovale. In rats, V1 and V2 enter the cranial compartment through the anterior lacerated foramen while V3 again enters through the foramen ovale. Ethmoidal (V1), nasopalatine (V2) and nasal (V2) branches of the trigeminal nerve provide sensory innervation to the nasal passages. The trigeminal sensory nerves project to trigeminal nuclei located in different positions within the brainstem and spinal cord. A portion of trigeminal ganglion cells with sensory endings located in the nasal epithelium also send collaterals directly into the olfactory bulb in addition to the brainstem.The trigeminal motor nucleus, located in the upper pons, contains the nuclei of motor neurons that travel in the small motor root to the muscles of mastication. The remaining three trigeminal nuclei mediate aspects of sensation. Of these, the principal sensory nucleus is located in the pons, lateral to the motor nucleus, the mesencephalic trigeminal nucleus reaches from the upper pons to the midbrain and the spinal trigeminal nucleus extends from the medulla down into the upper cervical spinal cord. Other nerves located in the nasal passages include the nervus terminalus (terminal nerve; cranial nerve zero) and the vomeronasal nerve and organ (Jacobsen's organ) although neither nerve has yet been implicated as providing a pathway for CNS drug delivery.

2.1.2.4 Vasculature of the nasal passages:

The nasal passages are highly vascular, an important feature mediating the absorption of many drugs into the systemic circulation. Blood supply to the nasal passages is principally provided by (i) branches of the ophthalmic artery: the anterior and posterior ethmoidal arteries (olfactory region, anterior septum, and anterior lateral wall), (ii) the sphenopalatine artery (mostly posterior septum and posterior lateral wall with smaller branches extending to further areas) and (iii) branches of the facial artery (antero-inferior septum and lateral wall); extensive anastomoses occur between each of these arteries in the antero-inferior portion of the septum known in humans as Kiesselbach's plexus (Little's area), a common site for nose bleeds. Venous drainage from the nasal passages of humans occurs principally through the sphenopalatine vein (posterior nasal passage) and veins accompanying the ethmoidal arteries (anterior nasal passage); some veins pass through the cribriform plate, joining others on the frontal lobe.

2.1.2.5 Pathways from the nasal passages to the central nervous system:

The precise pathways and mechanisms by which a drug travels from the nasal epithelium to various regions of the CNS have not been fully elucidated. The central distribution of [125I]-labeled proteins following IN administration in rats and monkeys has suggested that delivery occurs along olfactory and trigeminal nerve components in the nasal epithelium to the olfactory bulb and brainstem, respectively with further dispersion to other CNS areas from these initial points of brain entry. Atleast three sequential transport steps are therefore necessary for a substance to be delivered to distant, widespread sites within the CNS following IN administration: (1) transport across the epithelial 'barriers' (olfactory or respiratory) in the nasal passages, (2) transport from the nasal mucosa to sites of brain entry near the pial brain surface in the cranial compartment (i.e. entry points of peripheral olfactory or trigeminal nerve-associated components comprising the delivery pathways) and (3) transport from these initial brain entry sites to other sites within the CNS.

2.1.2.6 Transport across nasal epithelial barriers:

Transport across the 'barriers' presented by the olfactory or respiratory epithelia may occur either by intracellular or extracellular pathways. Intracellular pathways across the olfactory epithelium include endocytosis into OSN and subsequent intraneuronal transport to the olfactory bulb or transcytosis (i.e. transcellular transport) across sustentacular cells to the lamina propria as shown in Fig. 2.1A. OSN have the ability to endocytose certain viruses (e.g. herpes, poliomyelitis, rhabdo viruses) as well as large molecules such as horseradish peroxidase (HRP),wheat germ agglutinin-horseradish peroxidase (WGAHRP) and albumin from the nasal passages and then transport them intracellularly along the axon in the antero grade direction towards the olfactory bulb. HRP is taken up by OSN to a limited extent via fluid-phase endocytosis whereas WGA-HRP is internalized by OSN more avidly via adsorptive endocytosis. Intracellular pathways across the respiratory epithelium potentially include endocytosis into peripheral trigeminal nerve processes located near the epithelial surface and subsequent intracellular transport to the brainstem or transcytosis across other cells of the respiratory epithelium to the lamina propria (see Fig. 2.2A for relationships). Similar to what is observed in OSN, in WGA-HRP is internalized and transported intraneuronally within the trigeminal nerve to the brainstem. Viruses and bacteria may also be transmitted to the CNS along trigeminal nerve components within the nasal

passages. Extracellular transport pathways across either the olfactory or respiratory epithelia primarily include paracellular diffusion to the underlying lamina propria (e.g. as shown in Fig. 1.1A for the olfactory epithelium). In addition to its intracellular uptake by OSN, HRP has been shown to pass through open intercellular clefts to reach the olfactory bulb when applied intranasally in mice and squirrel monkeys.

The presence of TJ at an epithelial barrier will be the primary determinant of a given molecule's paracellular permeability. Significantly, the TJ proteins zonula occludens (ZO)-1, 2 and 3, occludin and claudins- 1, 3, 4, 5 and 19 are all expressed in the olfactory epithelium of rats. It has been suggested that the regular turnover of cells in the nasal epithelium may lead to continual rearrangement and loosening of the TJ, a consequence of resident basal cell populations dividing throughout life to replace OSN/sustentacular cells in the olfactory epithelium and ciliated/goblet cells in the respiratory epithelium. Although speculative, the replacement of cells throughout life may create similar potential spaces in both the olfactory and respiratory epithelia of the nasal passages, possibly facilitating paracellular transport of larger MW substances to the lamina propria.

2.1.2.7 Transport from the nasal mucosa to sites of brain entry:

Transport from the nasal mucosa to brain entry points at the level of the olfactory bulbs or brainstem occur via intracellular pathways (endocytosis and intraneuronal transport within OSN or trigeminal ganglion cells) or extracellular pathways (diffusion or convection within perineural, perivascular or lymphatic channels associated with olfactory and trigeminal nerve bundles extending from the lamina propria to the brain).

The possible fates of substances reaching the extracellular environment of the lamina propria are numerous and include: (1) absorption into blood vessels and entry into the general circulation; (2) absorption into lymphatic vessels draining to the deep cervical lymph nodes of the neck;(3) extracellular diffusion or convection in compartments associated with nerve bundles, particularly perineural or perivascular spaces, with

subsequent entry into the cranial compartment (Fig. 1.1A). Once a substance crosses the nasal epithelium into the lamina propria, it may be absorbed by the rich supply of nasal blood vessels and enter the systemic circulation. Drugs absorbed into the systemic circulation would then have to cross the BBB or blood–CSF barriers to reach the CNS. The nasal vasculature may therefore act as a sink for some IN applied substances, effectively preventing them from reaching the CNS. Although some nasal endothelial cells express TJ proteins such as ZO-1, occludin, and claudin-5, large capillaries of the lamina propria as well as smaller capillaries surrounding glands in the nasal respiratory epithelium possess fenestrations with porous basement membranes. Nasal venules and arterioles are continuous and lack fenestrations.

It has been reported that blood vessels in the lamina propria of the olfactory submucosa appear permeable to both lanthanum nitrate (MW=139 Da) and Evans blue (MW=961 Da). Many dyes and proteins administered intranasally may be recovered at least in part from the deep cervical lymph nodes in the neck. It has been known for well over 100 years that dyes injected into the CSF of the subarachnoid space will stain the perineural space of the olfactory nerve and drain through the nasal mucosa into the deep cervical lymph nodes.

Large MW compounds such as Evans blue-albumin or [125I]-albumin are concentrated in the perivascular spaces of the middle cerebral arteries and in the deep cervical lymph nodes after injection into CSF or brain. Microfil injections into the CSF compartment of human cadavers also show evidence of connections between CSF and nasal lymphatic vessels.

2.1.2.8 Transport from brain entry sites to other CNS areas:

Final distribution from drug entry points at the level of the olfactory bulb and brainstem to other areas of the CNS may be envisioned to occur either by intracellular transport (i.e. transfer and uptake to second order neurons synapsing with peripheral OSN or trigeminal ganglion cells) or extracellular transport (e.g. widespread distribution via convective transport within the cerebral perivascular spaces, local diffusion at the entry points and local diffusion from perivascular spaces into the parenchyma).

2.2 Introduction to drug (Venlafaxine HCl) [5]

Venlafaxine hydrochloride, structurally a novel antidepressant is designated (R/S)-1-[2-(dimethylamino)-1-(4-methoxy phenyl) ethyl] cyclohexanol hydrochloride OR (±)1-[a-[(dimethylamino) methyl] pmethoxy benzyl] cyclohexanol hydrochloride and has the empirical formula of C17H27NO2 HCl.

Venlafaxine, an antidepressant agent structurally unrelated to other antidepressants, is used to treat melancholia, generalized anxiety disorder (GAD), panic disorder, posttraumatic stress disorder and hot flashes in breast cancer survivors.

Preclinical studies have shown that venlafaxine and its active metabolite, O-desmethyl venlafaxine (ODV) are potent inhibitors of neuronal serotonin and nor epinephrine reuptake and weak inhibitors of dopamine reuptake. Venlafaxine and ODV have no significant affinity for muscarinic cholinergic, H1 –histaminergic or adrenergic receptors in vitro.

Venlafaxine is readily absorbed from the gastrointestinal tract, after oral doses it undergoes extensive first pass metabolism in the liver mainly to the active metabolite O-desmethylvenlafaxine; formation of o-desmethylvenlafaxine is mediated by the cytochrome p450 isoenzyme CVYP3D6. The isoenzyme CYP3A4 is also involved in the metabolism of venlafaxine.

Other metabolites include N-desmethylvenlafaxine and N,O-desmethylvenlafaxine. Peak plasma concentrations of venlafaxine and O-desmethylvenlafaxine appear about 2 and 4 hours after a dose, respectively. Venlafaxine is 27% and O-desmethylvenlafaxine 30% bound to plasma proteins. The mean elimination half life of venlafaxine and O-desmethylvenlafaxine is about 5 and 11 hours, respectively. Venlafaxine is excreted mainly in the urine, mainly in the form of its metabolites, either free or in conjugated form; about 2% is excreted in the faeces.

2.2.1 CAS : 93413-69-5 (Venlafaxine)

99300-78-4 (Venlafaxine Hydrochloride)

2.2.2 Structure of Venlafaxine HCl :

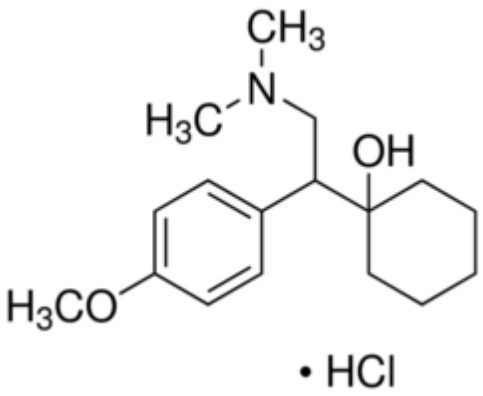

2.2.3 Physicochemical properties : [6-8]

- Name: Venlafaxine HCl
- I.U.P.A.C.Name: *RS*)1-[2-dimethylamino-1-(4-methoxyphenyl) ethyl] cyclohexanol hydrochloride.
- Molecular Formula: $C17H27NO_2$.
- Molecular Weight: 313.87.
- Physical and Chemical Properties: It is white crystalline solid having melting point 213-216°C, its predicted solubility is 572 mg/ml and Partition coefficient is 0.43. Its bioavailability is 40-45% and half life (5 ± 2 h) of parent compound and (10.43 ± 4.3 h) of active metabolite.
- Dose: 75 mg to 450 mg/day.

2.2.4 Mechanism of action: [9]

Venlafaxine is a bicyclic antidepressant and is usually categorized as a serotonin norepinephrine reuptake inhibitor (SNRI), but it has been referred to as a serotonin-norepinephrine-dopamine reuptake inhibitor (SNDRI).

It works by blocking the transporter "reuptake" proteins for key neurotransmitters affecting mood, thereby leaving more active neurotransmitters in the synapse.

The neurotransmitters affected are serotonin and norepinephrine. Additionally, in high doses it slightly inhibits the reuptake of dopamine.

2.2.5 Pharmacokinetics: [10]

A) Absorption

Venlafaxine is well absorbed, with at least 92% of an oral dose being absorbed into systemic circulation and absolute bioavailability is 45%. Steady-state concentrations of venlafaxine and O-desmethylvenlafaxine (ODV) in plasma are attained within 3 days of oral dosing. It exhibits linear kinetics over dose range of 75 to 450 mg/day. Food has no significant effect on the absorption of venlafaxine and on the formation of the O-desmethyl venlafaxine.

B) Distribution

Volume of distribution of venlafaxine is 7.5 L/kg (5.7 L/kg for ODV) 27% of venlafaxine and 30% of ODV is protein bound. Steady-state concentrations of venlafaxine and its metabolite are attained in the blood within 3 days and therapeutic effects are usually achieved within 3 to 4 weeks.

C) Metabolism

It is extensively metabolized in the liver via the CYP2D6 isoenzyme to desvenlafaxine (O-desmethylvenlafaxine), which is just as potent a serotonin-norepinephrine reuptake inhibitor as the parent compound, meaning that the differences in metabolism between extensive and poor metabolizers are not clinically important in terms of efficacy. Side effects, however, are reported to be more severe in CYP2D6 poor metabolizers.

D) Elimination

No accumulation of venlafaxine has been observed during chronic administration in healthy subjects. Renal elimination of venlafaxine and its metabolite is the primary route of excretion. Approximately 87% of the venlafaxine HCl is recovered in urine within 48 hrs. as either unchanged venlafaxine 5%, unconjugated o-desmethyl venlafaxine (29%), conjugated 0-desmethyl venlafaxine or other minor inactive metabolite. Elimination half-life of Venlafaxine is 5 hrs and 11 hour for active metabolite O-desmethyl Venlafaxine. The half-life of venlafaxine is relatively short,and therefore, patients are directed to adhere to a strict medication routine, avoiding missing a dose. Even a single missed dose can result in the withdrawal symptoms.

2.2.6 Uses and Administration: [5]

Depression: Clinical depression (unipolar depression) is a disturbance of mood that is distinguishable from the usual mood fluctuations of everyday life. A depressed mood is usually the major symptom, which may be accompanied by other mental or somatic symptoms representing several depressive symptoms. Suicide is a significant risk and upto half of all patients with depression may attempt suicide during their lifetime. Risk factors for developing depression include female gender and a positive family history. The decision to start treatment should be based on the severity and the risks to the patient.

Patients with mild depression may improve while being monitored without any additional help; in others simple interventions such as problem-solving, counseling, or exercise may be effective. The evidence for the efficacy of antidepressants in mild depression is lacking and initial treatment with antidepressants is not recommended, however patients with persistent mild depression or those with a history of depression may benefit from antidepressant treatment.

Patients with moderate depression should be treated with an antidepressant, in addition psychological treatments (particularly cognitive behavioural therapy) are also effective.

A combination of antidepressants and psychological treatments should be considered in patients with severe depression. ECT may also be of value, particularly when a rapid

improvement of symptoms is essential (in patients with high risk of suicide) or in patients with depressive psychosis or psychomotor retardation.

For patients with psychotic depression, an antipsychotic may be required in addition to any antidepressant treatment, ECT should also be considered.

Light therapy appears to be effective in patients with seasonal affective disorder. Exposure to bright artificial light may take place at any time of the day and the therapy should continue until the natural seasonal remission of the disorder; antidepressants drugs may also be used.

Venlafaxine is given by mouth as the hydrochloride although doses are expressed in terms of the base; venlafaxine hydrochloride 28.3 mg is equivalent to about 25 mg of venlafaxine.

Venlafaxine is used in the treatment of depression. The initial daily dose is equivalent to venlafaxine 75 mg in two or three divided doses with food. In the USA, it is suggested that some patients may be best started on 37.5 mg daily for the first 4 to 7 days before increasing the dose to 75 mg daily. The dose may be increased, if necessary, after several weeks to 150 mg daily. Further increases, to a maximum daily dose of 375 mg, may be made in increaments of upto 75 mg at intervals of atleast 2 to 4 days. Such doses may be required in severly depressed or hospotalised patients and should be gradually reduced to minimum effective dose. Modified released preparations are available for once daily dosing.

Venlafaxine is also used, as a modified release preparation, in the treatment of generalized anxiety disorder. The recommended initial dose is 75 mg once daily by mouth. In the USA it is suggested that some patients may be best begun with 37.5 mg daily for 4 to 7 days initially; dosage may subsequently be adjusted in increaments of upto 75 mg, at intervals of atleast 4 days, to a maximum of 225 mg daily. Venlafaxine should be withdrawn gradually if there is no response after 8 weeks.

Reduced doses may need to be given in hepatic or renal impairment.

Venlafaxine should be withdrawn gradually to reduce the risk of withdrawal symptoms.

Administration in hepatic impairment: [5]

UK licensed drug information considers that patients with mild hepatic impairment donot require change in dose of venlafaxine. For those with moderate impairment, the dose should be reduced by half and given once daily. There are insufficient data to make any recommendations for patients with severe impairment.

Administration in renal impairment: [5]

The UK licensed drug information states that, based on glonerular filtration rate (GFR), patients with mild renal impairment (GFR above 30 ml/minute) donot require a change in dose of venlafaxine. For those with moderate impairment (GFR 10 to 30 ml/minute). The dose should be reduced by 50% and once-daaily dosage may be appropriate. There are insufficient data to make any recommendation for patients with severe impairment GFR less than 10 ml/minute).

In the USA, it is recommended that patients with a GFR of 10 to 70 ml/minute reduce the dose of immediate-release venlafaxine by 25% and of modified relese venlafaxine by 25 to 50%; regardless of preparation, in those undergoing haemodialyses, the dose should be reduced by 50% and withheld until the dialysis is completed.

Anxiety disorders:

Venlafaxine is used in the treatment of generalized anxiety disorder and social anxiety disorder, it may also be used in a variety of other types of anxiety disorders, including the treatment of obsessive-compulsive disorder, panic disorder and post-traumatic stress disorder.

2.2.7 Contraindication:

Venlafaxine is not recommended in patients hypersensitive to it, nor should it be taken by anyone who is allergic to the inactive ingredients, which include gelatine, cellulose, ethyl cellulose, iron oxide, titanium dioxide and hypromellose. It should never be used with a monoamine oxidase inhibitor (MAOI), as it can cause potentially fatal. Venlafaxine can increase eye pressure, so those with glaucoma may require more frequent eye checks.

Pregnant women:

Venlafaxine should only be used during pregnancy if clearly needed. Prospective studies have not shown any statistically significant congenital malformations. There have, however, been some reports of self-limiting effects on new-born infants. As with other serotonin reuptake inhibitors, these effects are generally short-lived, lasting only 3 to 5 days and rarely resulting in severe complications.

Suicide:

The US Food and Drug Administration body (FDA) requires all antidepressants, including venlafaxine, to carry a black box warning with a generic warning about a possible suicide risk. In addition, the most recent research indicated that patients taking venlafaxine are at increased risk of suicide.

2.1.8 Common side effects:

Sexual dysfunction is often a side effect of drugs that inhibit serotonin reuptake. Specifically, common side effects include difficulty becoming aroused, lack of interest in sex and anorgasmia (trouble achieving orgasm), loss of or decreased response to sexual stimuli and ejaculatory anhedonia are also possible. Although usually reversible, there are some who report sexual side effects persisting after the drug have been withdrawn. This is known as post-SSRI sexual dysfunction. Other side effects are like headache, chest pain, trauma, vasodilation, increased blood pressure/hypertension, tachycardia, postural hypotension, rash, itching, diarrhoea, upset stomach or indigestion (dyspepsia), flatulence, hypertonia mydriasis, hair loss are reported.

2.1.9 Discontinuation syndrome:

Patients stopping venlafaxine commonly experience SSRI discontinuation syndrome, i.e. withdrawal symptoms. Such symptoms may occur when abruptly ceasing the medication, decreasing one's dose too quickly, or even after missing a regular dose. Withdrawal symptoms may include agitation, anorexia, anxiety, confusion, impaired coordination, diarrhoea, dizziness, dry mouth, dysphoric mood, fasciculation, fatigue, headaches, hypomania, insomnia, nausea, nervousness, nightmares, sensory disturbances (including shock-like electrical sensations), somnolence, sweating, tremor, vertigo, and vomiting. The high risk of discontinuation syndrome symptoms

may reflect venlafaxine's short half-life missing even a single dose can induce discontinuation effects in some patients.

2.1.10 Drug interactions:

Venlafaxine may lower the seizure threshold, and co-administration with other drugs that lower the seizure threshold such as bupropion and tramadol should be done with caution and at low doses. There have been false positive phencyclidine (PCP) results caused by larger doses of venlafaxine, with certain on-site routine urine-based drug tests. Although the synergistic effects may not be as bad as with other antidepressants, it is still not recommended to take venlafaxine with alcohol.

2.1.11 Overdose:

Most patients overdosing with venlafaxine develop only mild symptoms. However, severe toxicity is reported, with the most common symptoms being CNS depression, serotonin toxicity, seizure or cardiac conduction abnormalities. Venlafaxine's toxicity appears to be higher than other SSRIs, with a fatal toxic dose closer to that of the tricyclic antidepressants than the SSRIs. Doses of 900 mg or more are likely to cause moderate toxicity. Deaths have been reported following very large doses. Plasma venlafaxine concentrations in overdose survivors have ranged from 6 to 24 mg/l, while post-mortem blood levels in fatalities are often in the 10–90 mg/l range.

Management of overdose:

There is no specific antidote for venlafaxine, and management is generally supportive, providing treatment for the immediate symptoms. Administration of activated charcoal can prevent absorption of the drug. Monitoring of cardiac rhythm and vital signs is indicated. Seizures are managed with benzodiazepines or other anticonvulsants. Forced diuresis, hemodialysis, exchange transfusion, or hemoperfusion are unlikely to be of benefit in hastening the removal of venlafaxine, due to the drug's high volume of distribution.

2.3 Introduction to Excipients

1) Pectin [11]

Pectin is a naturally occurring biopolymer that is finding increasing applications in the pharmaceutical and biotechnology industry. It has been used successfully for many years in the food and beverage industry as a thickening agent, a gelling agent and a colloidal stabiliser. Pectin also has several unique properties that have enabled it to be used as a matrix for the entrapment and/or delivery of a variety of drugs, proteins and cells.

Chemistry of pectin:

Source and production:[11]

Pectin is a complex mixture of polysaccharides that makes up about one third of the cell wall dry substance of higher plants. Much smaller proportions of these substances are found in the cell walls of grasses. The highest concentrations of pectin are found in the middle lamella of cell wall, with a gradual decrease as one passes through the primary wall toward the plasma membrane. Although pectin occurs commonly in most of the plant tissues, the number of sources that may be used for the commercial manufacture of pectins is very limited. Because the ability of pectins to form gel depends on the molecular size and degree of esterification (DE), the pectin from different sources does not have the same gelling ability due to variations in these parameters. At present, commercial pectins are almost exclusively derived from citrus peel or apple pomace, both by-products from juice (or cider) manufacturing. Apple pomace contains 10-15% of pectin on a dry matter basis. Citrus peel contains of 20-30%. From an application point of view, citrus and apple pectins are largely equivalent. Citrus pectins are light cream or light tan in colour; apple pectins are often darker.

Alternative sources include sugar beet waste from sugar manufacturing, sunflower heads (seeds used for edible oil), and mango waste. Commercially, pectin is extracted by treating the raw material with hot dilute mineral acid at pH about 2. The precise length of extraction time varies with raw material, the type of pectin desired, and from one manufacturer to another. The hot pectin extract is separated from the solid residue

as efficiently as possible. This is not easy since the solids are by now soft and the liquid phase are viscous. The viscosity increases with pectin concentration and molecular weight. The pectin extract may be further clarified by filtration through a filter aid. The clarified extract is then concentrated under vacuum. Powdered pectin can be produced by mixing the concentrated liquid from either apple or citrus with an alcohol (usually isopropanol). The pectin is separated as a stringy gelatinous mass, which is pressed and washed to remove the mother liquor, dried and ground. This process yields pectin of around 70% esterification (or methoxylation). To produce other types, some of the ester groups must be hydrolysed. This is commonly carried out by the action of acid, either before or during a prolonged extraction, in the concentrated liquid, or in alcoholic slurry before separation and drying. This process can produce a range of calcium reactive low methoxyl pectins. Hydrolysis using ammonia results in the conversion of some of the ester groups into amide groups, producing amidated low methoxyl pectins.

Chemical structure:

Pectin is an essentially linear polysaccharide. Like most other plant polysaccharides, it is both polydisperse and polymolecular and its composition varies with the source and the conditions applied during isolation. The composition and structure of pectin are still not completely understood although pectin was discovered over 200 years ago. The structure of pectin is very difficult to determine because pectin can change during isolation from plants, storage, and processing of plant material. In addition, impurities can accompany the main components. At present, pectin is thought to consist mainly of D-galacturonic acid (GalA) units, joined in chains by means of á-(1-4) glycosidic linkage. These uronic acids have carboxyl groups, some of which are naturally present as methyl esters and others which are commercially treated with ammonia to produce carboxamide groups.

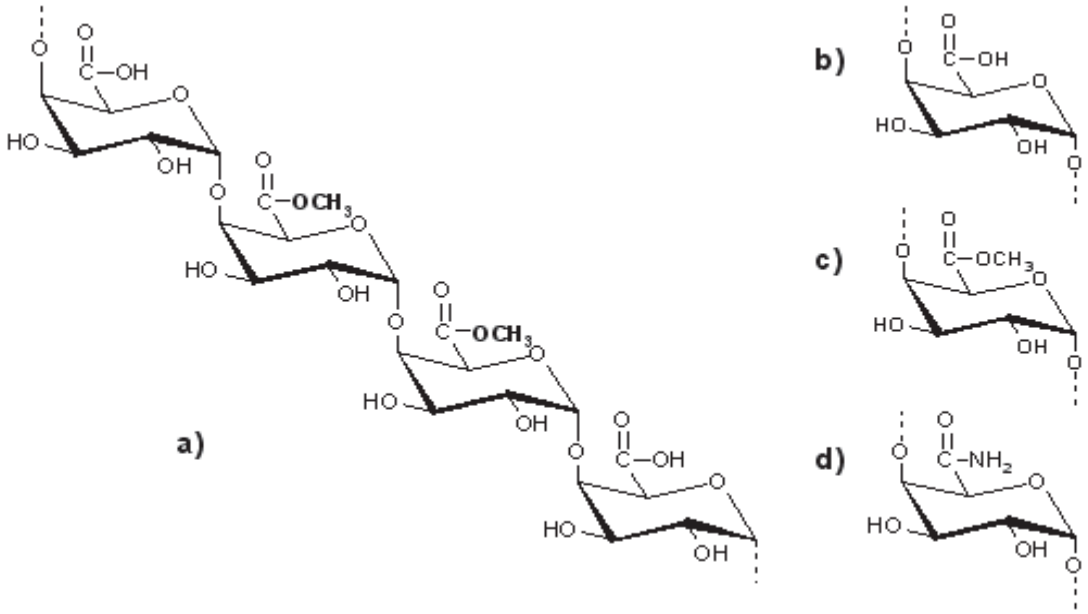

Fig. 2.3 (a) A repeating segment of pectin molecule and functional groups: (b) carboxyl; (c) ester; (d) amide in pectin chain.[11]

Pectin contains from a few hundred to about 1000 saccharide units in a chain-like configuration; this corresponds to average molecular weights from about 50,000 to 150,000 daltons. Large differences may exist between samples and between molecules within a sample and estimates may differ between methods of measurement.

In addition to the galacturonan segments shown in figure 2.3, neutral sugars are also present. Rhamnose (Rha) is a minor component of the pectin backbone and introduces a kink into the straight chain and other neutral sugars such as arabinose, galactose and xylose occur in the side chains. A chain of several hundred á-(1-4)-bonded GalA units with a varied DE is a typical fragment.

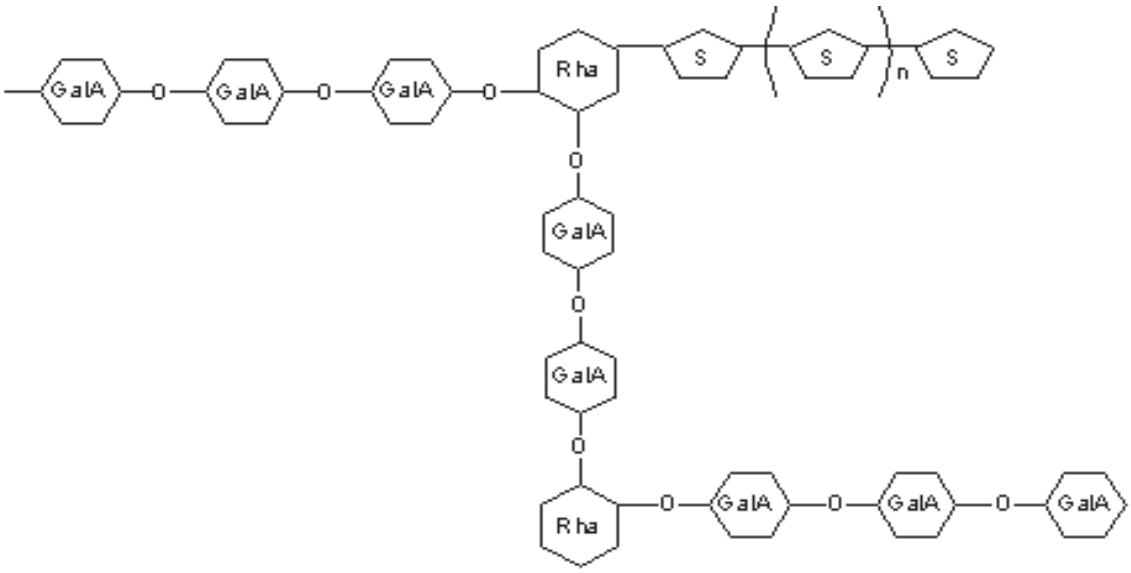

Fig. 2.4 Schematic diagram showing how rhamnose (Rha) insertions cause linking of galacturonic acid (GalA) chain; S = neutral sugars[11]

General properties of pectin:

- Pectin is a solid powder, off white in color.
- Pectin is practically odorless. It is mucilaginous.
- Pectin is stable at ordinary conditions, becomes unstable in excess heat. Pectin is soluble in pure water, partially soluble in cold water. It is insoluble in alcohol and organic solvents. When pectin is mixed with alcohol or organic solvent and mixed with water it is soluble, whereas di- and tri- salts are weakly soluble or insoluble.
- Pectin is combustible at higher temperatures, because of this it must be kept away from heat and any source of ignition.
- Dry powdered pectin, when added to water, has a tendency to hydrate, very rapidly, forming gels.
- Dilute solutions are newtonian, but at a moderate concentration, they exhibit non-newtonian, pseudo plastic behavior characteristics.
- Viscosity, solubility and gelation are generally related (e.g. factors that increase gel strength will increase the tendency to gel, decrease solubility, and increase viscosity and vice versa).
- Coulombic repulsion is present between the carboxylate anions which prevent the aggregation of the polymer chains.

- Another property of pectin which plays a major role in most of its applications is its pH. When pH is lowered, ionization of carboxylate groups is suppressed, and this results in reduction in hydration of carboxylic acid groups. At higher pH the degree of methylation will be greater. At a pH of 5-6 low methoxylated pectin is stable, but high methoxylated pectin is stable only at room temperature.
- Pectin does not undergo polymerization but undergoes depolymerisation. Depolymerisation occurs when pectin molecules are treated with dilute acids at higher temperatures. They break into smaller fragments. The pectin which is dissolved in solutions gets decomposed spontaneously by deesterification as well as by depolymerisation. These rates depend upon the pH and on temperature. Deesterification is favored by low pH. Maximum stability of pectin occurs only at pH 4.
- The other properties which influence the wide spread applications of pectin are, degree of methoxylation, degree of esterification and degree of amidation.
- Generally pectin is valued by the pectin grade, defined as number of pounds of sugar that one pound of pectin can carry in a jelly.

Gel formation properties of pectin:

The most important use of pectin is based on its ability to form gels. HM-pectin forms gels with sugar and acid. This can be seen as a partial dehydration of the pectin molecule to a degree where it is in a state between fully dissolved and precipitated. The particular structure of pectin imposes some specific constraints. HM-pectin, unlike LM-pectin, does not contain sufficient acid groups to gel or precipitate with calcium ions, although other ions such as aluminium or copper cause precipitation under certain conditions. It has been suggested by Oakenfull (1991) that hydrogen bonding and hydrophobic interactions are important forces in the aggregation of pectin molecules. Gel formation is caused by hydrogen bonding between free carboxyl groups on the pectin molecules and also between the hydroxyl groups of neighbouring molecules. In a neutral or only slightly acid dispersion of pectin molecules, most of the unesterified carboxyl groups are present as partially ionised salts. Those that are ionised produce a negative charge on the molecule, which together with the hydroxyl groups causes it to attract layers of water. The repulsive forces between these groups, due to their negative

charge, can be sufficiently strong to prevent the formation of a pectin network. When acid is added, the carboxyl ions are converted to mostly unionised carboxylic acid groups. This decrease in the number of negative charges not only lowers the attraction between pectin and water molecules, but also lowers the repulsive forces between pectin molecules. Sugar further decreases hydration of the pectin by competing for water. These conditions decrease the ability of pectin to stay in a dispersed state. When cooled, the unstable dispersing of less hydrated pectin forms a gel, a continuous network of pectin holding the aqueous solution. The rate at which gel formation takes place is also affected by the degree of esterification. A higher DE causes more rapid setting. Rapid-set pectins (i.e. pectin with a DE of above 72%) also gel at lower soluble solids and higher levels than slow-set pectins (i.e. pectin with a DE of 58-65%). LM-pectins require the presence of divalent cations (usually calcium) for proper gel formation. The mechanism of LM-pectin gelation relies mainly on the well-known 'egg-box' model. The mechanism involves junction zones created by the ordered, side-by-side associations of galacturonans, whereby specific sequences of GalA monomer in parallel or adjacent chains are linked intermolecularly through electrostatic and ionic bonding of carboxyl groups.

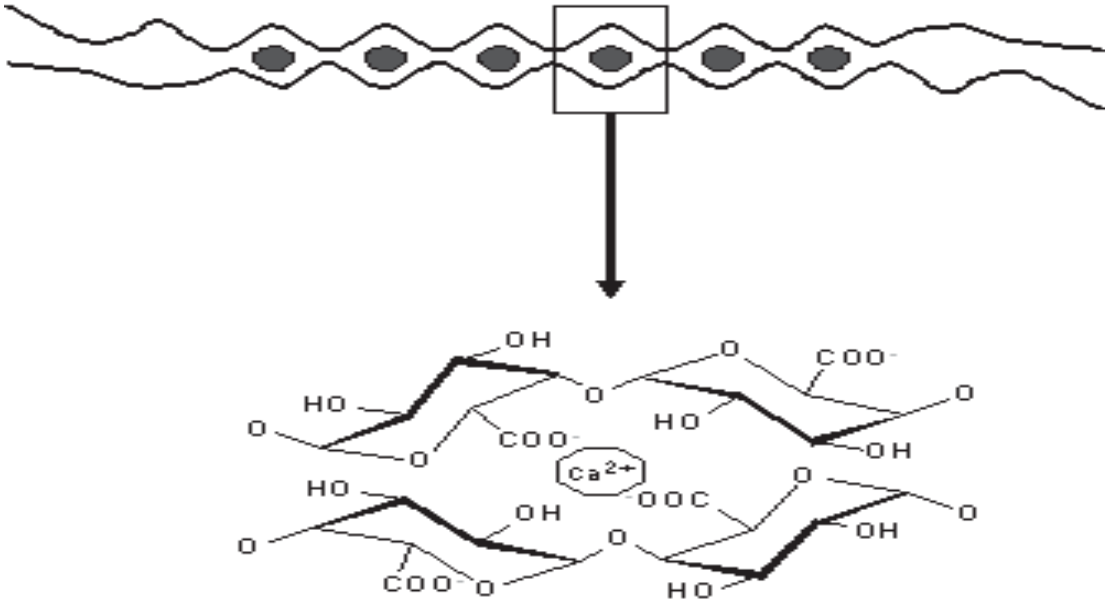

Fig. 2.5 Schematic representation of calcium binding to polygalactoronate sequences: 'egg box' dimer and 'egg-box' cavity[11]

The gel structure is a net-like formation of cross-linked pectin molecules. The cross-linkages formed by ionic bonds between the carboxyls are strong and produce a rather brittle, less elastic than those formed by hydrogen bonding as in regular pectin. With pectins of lower DE, there is an increasing probability for the formation of cross-links with a given amount of calcium. As the number of reactive carboxyl groups that can form a salt bridge increases, the greater the chances are that the bridge will be formed. Furthermore, because of the larger amount of charged groups, de-esterified molecules are straighter than the esterified ones, so they will be more likely to form calcium linkages.

Pharmaceutical uses of pectin:

Pectin has applications in the pharmaceutical industry. Pectin favaorably influences cholesterol levels in blood. It has been reported to help reduce blood cholesterol in a wide variety of subjects and experimental conditions as comprehensively reviewed. Consumption of at least 6 g/day of pectin is necessary to have a significant effect in cholesterol reduction. Amounts less than 6 g/day of pectin are not effective. Pectin acts as a natural prophylactic substance against poisoning with toxic cations. It has been shown to be effective in removing lead and mercury from the gastrointestinal tract and respiratory organs. When injected intravenously, pectin shortens the coagulation time of drawn blood, thus being useful in controlling hemorrhage or local bleeding. Pectin and combinations of pectin with other colloids have been used extensively to treat diarrheal diseases, especially in infants and children. Although a bactericidal action of pectin has been proposed to explain the effectiveness of pectin treating diarrhea, most experimental results do not support this theory. However, some evidence suggests that under certain in-vitro conditions, pectin may have a light antimicrobial action toward *Echerichia coli.*

Pectin reduces rate of digestion by immobilising food components in the intestine. This results in less absorption of food. The thickness of the pectin layer influences the absorption by prohibiting contact between the intestinal enzyme and the food, thus reducing the latter’s availability. Due to its large water binding capacity, pectin gives a feeling of satiety, thus reducing food consumption.

Since pectin can react with calcium ions, calcium pectinate has been investigated as an insoluble hydrophilic coating for sustained release delivery by interfacial complexation process.

Pectin has a promising pharmaceutical uses and is presently considered as a carrier material in colon-specific drug delivery systems (for systemic action or a topical treatment of diseases such as ulcerative colitis, Crohn's disease, colon carcinomas). The rationale for this is that pectin and calcium pectinate will be degraded by colonic pectinolytic enzymes, but will retard drug release in the upper gastrointestinal tract due to its insolubility and because it is not degraded by gastric or intestinal enzymes.

Pectin is an interesting candidate for pharmaceutical use, e.g. as a carrier of a variety of drugs for controlled release applications. Many techniques have been used to manufacture the pectin-based delivery systems, especially ionotropic gelation and gel coating. These simple techniques, together with the very safe toxicity profile, make pectin an exciting and promising excipient for the pharmaceutical industry for present and future applications.

2) Magnesium Chloride [6-8]

Nonproprietary Names:

USP: Magnesium Chloride

EP: Magnesii Chloridum Hexahydricum

BP: Magnesium Chloride Hexahydrate

Synonyms:

Magnesii chloridum

Magnesium chloritum

Chemical Name and CAS Registry Number:

Magnesium chloride anhydrous 7786-30-3

Magnesium chloride Hexahydrate 7791-18-6

Empirical Formula and Molecular Weight:

$MgCl_2$ anhydrous: 98.21

$MgCl_2$ Hexahydrate: 203.3

Functional Category:

Food additive

Mineral supplement

Used in electrolyte solutions

Applications in Pharmaceutical Formulation or Technology:

The main applications of magnesium chloride as an excipient relate to its dehydrating properties and, therefore, it has been used as an antimicrobial preservative, as a desiccant. Therapeutically, magnesium chloride injection 10% (as the dehydrate form) is used to treat low magnesium levels.

Description:

Colourless, odourless, deliquescent flakes or crystals, which loose water when heated to 100^{o}C. Very soluble in water, freely soluble in alcohol. pH of 5% solution in water is 4.5-7.

Stability and Storage Conditions:

Magnesium chloride is chemically stable; however, it should be protected from moisture. Store in airtight containers in a cool, dry place.

Regulatory Status:

GRAS listed. Included in the FDA inactive ingredients database (injections, ophthalmic preparations, suspensions, creams). Included in medicines licensed in the UK (eye drops; intraocular irrigation; vaccines; injection powders for reconstitution; nebulizer solution).

3) Calcium Chloride [6-8]

Nonproprietary Names:

BP: Calcium Chloride Dihydrate
Calcium Chloride Hexahydrate
JP: Calcium Chloride Hydrate
PhEur: Calcium Chloride Dihydrate
Calcium Chloride Hexahydrate
USP-NF: Calcium Chloride

Synonyms:

Calcii chloridum dihydricum
Calcii chloridum hexahydricum

Chemical Name and CAS Registry Number:

Calcium chloride anhydrous [10043-52-4]
Calcium chloride dihydrate [10035-04-8]
Calcium chloride hexahydrate [7774-34-7]

Empirical Formula and Molecular Weight:

$CaCl_2$ 110.98 (for anhydrous)
$CaCl_2.2H_2O$ 147.0 (for dihydrate)
$CaCl_2.6H_2O$ 219.1 (for hexahydrate)

Functional Category:

Antimicrobial preservative
Therapeutic agent
Water-absorbing agent.

Applications in Pharmaceutical Formulation or Technology:

The main applications of calcium chloride as an excipient relate to its dehydrating properties and, therefore, it has been used as an antimicrobial preservative, as a desiccant, and as an astringent in eye lotions. Therapeutically, calcium chloride injection 10% (as the dihydrate
form) is used to treat hypocalcemia.

Description:

Calcium chloride occurs as a white or colorless crystalline powder, granules, or crystalline mass, and is hygroscopic (deliquescent).

Table 2.3: Pharmacopeial specifications for calcium chloride.

Test	JP XV	PhEur 6.0	USP32–NF27
Identification	+	+	+
Appearance of solution	-	+	-
Acidity or alkalinity	+	+	-
Sulfates dihydrate— hexahydrate	40.024% -	4300 ppm 4200 ppm	- -
Aluminum Aluminum (for hemodialysis only) dihydrate - hexahydrate	-	41 ppm	1 mg/g
Iron, aluminum and phosphate	+	-	+
Barium	+	+	-
Iron dihydrate - hexahydrate	- -	410 ppm 47 ppm	- -
Heavy metals dihydrate - hexahydrate	410 ppm -	420 ppm 415 ppm	40.001% -
Magnesium and alkali salts dihydrate	-	40.5%	41.0%
Hypochlorite	+	-	-
Arsenic	42 ppm	-	-
Assay dihydrate hexahydrate	96.7–103.3% -	97.0–103.0% 97.0–103.0%	99.0–107.0% -

Typical Properties:

Acidity/alkalinity pH : 4.5–9.2 (5% w/v aqueous solution)

Boiling point : >160^{o}C (anhydrous)

Density (bulk) : 0.835 g/cm^{3} (dihydrate)

Melting point : 172^{o}C (anhydrous); 176^{o}C (dihydrate); 308^{o}C (hexahydrate).

Solidification temperature : 28.5–30^{0}C (hexahydrate)

Solubility : Freely soluble in water and ethanol (95%); insoluble in diethyl ether.

Stability and Storage Conditions:

Calcium chloride is chemically stable; however, it should be protected from moisture. Store in airtight containers in a cool, dry place.

Incompatibilities:

Calcium chloride is incompatible with soluble carbonates, phosphates, sulfates and tartrates. It reacts violently with bromine trifluoride, and a reaction with zinc releases explosive hydrogen gas. It has an exothermic reaction with water, and when heated to decomposition it emits toxic fumes of chlorine.

Regulatory Status:

GRAS listed. Included in the FDA inactive ingredients Database (injections, ophthalmic preparations, suspensions, creams). Included in medicines licensed in the UK (eye drops; intraocular irrigation; vaccines; injection powders for reconstitution; nebulizer solution; oral suspension).

4) Zinc Chloride [6-8]

Nonproprietary Names:

USP: Zinc Chloride

EP: Zincii chloridum

Synonyms:

Cinko chloridas
Zinci chloridum
Zincum chloratum

Chemical Name and CAS Registry Number:

Zinc chloride anhydrous 7646-85-7

Empirical Formula and Molecular Weight:

$ZnCl_2$: 136.3

Functional Category:

Food additive

Mineral supplement

Used in electrolyte solution

Applications in Pharmaceutical Formulation or Technology:

The main applications of zinc chloride as an excipient relate to its dehydrating properties and, therefore, it has been used as an antimicrobial preservative, as a desiccant. Therapeutically, zinc chloride injection 1% (as the dehydrate form) is used in electrolyte solutions.

Description:

A white or practically white, deliquescent crystalline powder. Very soluble in water. Freely soluble in alcohol and in glycerol. pH of 10% solution is 4.6-5.5.

Stability and Storage Conditions:

It should be protected from moisture. Store in non metallic containers.

Regulatory Status:

GRAS listed. Included in the FDA inactive ingredients database (injections, ophthalmic preparations, suspensions, creams).

5) Poloxamer [6-8, 12]

Nonproprietary Names:

BP : Poloxamers

PhEur : Poloxamera

USPNF : Poloxamer

Synonyms:

Monolan

Pluroni

Poloxalkol

Polyethylene–propylene glycol copolymer

Polyoxyethylene–polyoxy propylene copolymer,

Supronic

Synperonic.

Lutrol

Chemical Name and CAS Registry Number:

a-Hydro-o-hydroxypoly(oxyethylene)poly(oxypropylene)poly(oxyethylene) block copolymer [9003-11-6]

Empirical Formula and Molecular Weight:

The poloxamer polyols are a series of closely related block copolymers of ethylene oxide and propylene oxide conforming to the general formula HO(C2H4O)a(C3H6O)b(C2H4O)aH.

Structural Formula:

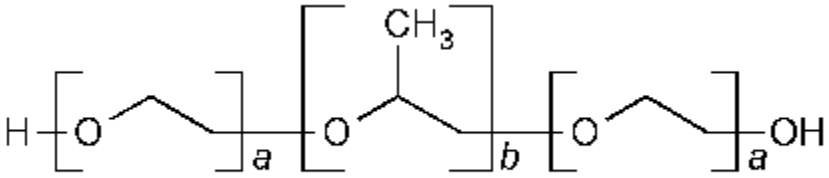

Table 2.4 : Typical poloxamer grades.

Poloxamer	Physical form	a	b	Average molecular weight
124	Liquid	12	20	360
188	Solid	80	27	510
237	Solid	64	37	830
338	Solid	141	44	400
407	Solid	101	56	600

Functional Category:

Dispersing agent

Emulsifying and coemulsifying agent

Solubilizing agent

Tablet lubricant

Wetting agent.

Description:

Poloxamers generally occur as white, waxy, free-flowing prilled granules, or as cast solids. They are practically odorless and tasteless. At room temperature, poloxamer 124 occurs as a colorless liquid.

Applications in Pharmaceutical Formulation or Technology:

Poloxamers are nonionic polyoxyethylene–polyoxypropylene copolymers used primarily in pharmaceutical formulations as emulsifying or solubilizing agents. The polyoxyethylene segment is hydrophilic while the polyoxypropylene segment is hydrophobic. All of the poloxamers are chemically similar in composition, differing only in the relative amounts of propylene and ethylene oxides added during manufacture. Their physical and surface-active properties vary over a wide range and a number of different types are commercially available; Poloxamers are used as emulsifying agents in intravenous fat emulsions and as solubilizing and stabilizing agents to maintain the clarity of elixirs and syrups. Poloxamers may also be used as wetting agents in ointments, suppository bases, and gels; and as tablet binders and coatings. Poloxamer 188 has also been used as an emulsifying agent for fluorocarbons used as artificial blood substitutes and in the preparation of solid-dispersion systems. More recently, poloxamers have found use in drug-delivery systems. Therapeutically, poloxamer 188 is administered orally as a wetting agent and stool lubricant in the treatment of constipation; it is usually used in combination with a laxative such as danthron. Poloxamers may also be used therapeutically as wetting agents in eye-drop formulations, in the treatment of kidney stones, and as skin-wound cleansers. Poloxamer 338 and 407 are used in solutions for contact lens care.

Table 2.5 Uses of poloxamer

Use	Concentration (%)
Fat emulsifier	0.3
Flavor solubilizer	0.3
Fluorocarbon emulsifier	2.5
Gelling agent	15-50
Spreading agent	1
Suppository base	1-5

Tablet coating	4-6
Tablet excipient	10
Wetting agent	5-10

Table 2.6: Pharmacopeial specifications for poloxamer

Test	**PhEur 2005**	**USPNF 23**
Identification	+	-
Appearance of solution	+	-
Average molecular weight For poloxamer 124	2 090–2 360	2 090-2 360
For poloxamer 188	7 680–9 510	7 680-9 510
For poloxamer 237	6 840–8 830	6 840-8 830
For poloxamer 338	12 700–17 400	12 700-17 400
For poloxamer 407	9 840–14 600	9 840-14 600
Weight percent oxyethylene For poloxamer 124	71.5–74.9	73.2±1.7
For poloxamer 188	79.9–83.7	81.8±1.9
For poloxamer 237	70.5–74.3	72.4±1.9
For poloxamer 338	81.4–84.9	83.1±1.7
For poloxamer 407	71.5–74.9	73.2±1.7
pH (aqueous solution)	5.0–7.5	5.0±7.5
Unsaturation (mEq/g) For poloxamer 124	-	0.020±0.008
For poloxamer 188	-	0.026±0.008
For poloxamer 237	-	0.034±0.008
For poloxamer 338	-	0.031±0.008
For poloxamer 407	-	0.048±0.017
Oxypropylene:oxyethylene Ratio	+	-
Total ash	40.4%	-
Heavy metals	-	40.002%

Organic volatile impurities	-	+
Water	41.0%	-
Free ethylene oxide, propylene oxide and 1,4-dioxane	+	+
Ethylene oxide	-	<1 ppm
Propylene oxide	-	<5 ppm
1,4-Dioxane	-	<5 ppm

Typical Properties:

Acidity/alkalinity pH : 5.0–7.4 for a 2.5% w/v aqueous solution.

Cloud point: >100^{o}C for a 1% w/v aqueous solution, and a 10% w/v aqueous solution of poloxamer 188.

Density : 1.06 g/cm^{3} at 258^{o}C

Flash point : 260^{o}C

Flowability : solid poloxamers are free flowing.

HLB value : 0.5–30; 29 for poloxamer 188.

Melting point : 16^{o}C for poloxamer 124;

52–57^{o}C for poloxamer 188;

49^{o}C for poloxamer 237;

57^{o}C for poloxamer 338;

52–57^{o}C for poloxamer 407.

Moisture content : poloxamers generally contain less than 0.5% w/w water and are hygroscopic only at relative humidity greater than 80%.

Solubility: solubility varies according to the poloxamer type.

Table 2.7: Solubility of various grades of poloxamer

Type	**Solvent**				
	Ethanol (95%)	**Propan-2-ol**	**Propylene glycol**	**Water**	**Xylene**
Poloxamer 124	Freely	Freely	Freely	Freely	Freely

	soluble	soluble	soluble	soluble	soluble
Poloxamer 188	Freely soluble	-	-	Freely soluble	-
Poloxamer 237	Freely soluble	Sparingly soluble	-	Freely soluble	Sparingly soluble
Poloxamer 338	Freely soluble	-	Sparingly soluble	Freely soluble	-
Poloxamer 407	Freely soluble	Freely soluble	-	Freely soluble	-

Surface tension:

19.8 mN/m (19.8 dynes/cm) for a 0.1% w/v aqueous poloxamer 188 solution at 258^{o}C;
24.0 mN/m (24.0 dynes/cm) for a 0.01% w/v aqueous poloxamer 188 solution at 258^{o}C;
26.0 mN/m (26.0 dynes/cm) for a 0.001% w/v aqueous poloxamer solution at 258^{o}C.

Viscosity (dynamic):

1000 mPa s (1000 cP) for poloxamer 188.

Stability and Storage Conditions:

Poloxamers are stable materials. Aqueous solutions are stable in the presence of acids, alkalis, and metal ions. However, aqueous solutions support mold growth. The bulk material should be stored in a well-closed container in a cool, dry place.

Incompatibilities:

Depending on the relative concentrations, poloxamer 188 is incompatible with phenols and parabens.

Regulatory Status:

Included in the FDA Inactive Ingredients Guide (IV injections; inhalations, ophthalmic preparations; oral powders, solutions, suspensions, and syrups; topical preparations). Included in non parenteral medicines licensed in the UK. Included in the Canadian List of Acceptable Non-medicinal Ingredients.

3.1 Literature review on venlafaxine hydrochloride

Thorat et. al[13] provides the initial release of the drug sufficient to provide a therapeutic dose soon after administration and then a gradual release over an extended period. Recently, Sustained release dosage forms became a very useful tool in medical practice offering a wide range of actual and perceived advantages to the patients. The basic rational for sustained drug delivery is to alter the drug release and also to formulate such dosage form that improves patient compliance. To target chronic diseases it is the best suitable dosage form. An appropriate formulation can make the absorption, distribution, metabolism and elimination (ADME) profile of a drug much more favourable. Venlafaxine HCl is an orally active serotonin noradrenalin reuptake inhibitor used in the treatment of major depressive disorders. The successful treatment of depression depends on the maintenance of effective drug concentration level in the body for which a constant and uniform supply of drug is desired. It is a highly water soluble drug (Class I) with the biological half life of 5 Hrs thus requires two to three time daily dosing to maintain plasma drug concentration. So providing its slow release to maintain therapeutic level is the major need of this formulation.The drug has elimination half life of 5(±2) hours shows that it is a suitable candidate for sustained release formulation. Advantage of this formulation over others is that it is easy to prepare and cost effective. Optimum concentration of Carbopol 971P and Ethyl cellulose based formulations was found to provide the desired release (95.47%) with a reduced frequency of administration. Release Kinetics shows it follws Korsmeyer Peppas model and mechanism is diffusion controlled or Fickian type. Thus, the Objective of the project was to formulate a sustained release matrix type tablet of Venlafaxine Hydrochloride meant for once-a-day administration.

Pund et. al[14] analysed kinetics studies for venlafaxine. Since the nose-to-brain pathway has been indicated for delivering drugs to the brain, they analyzed the transport of venlafaxine through sheep nasal mucosa. Transmucosal permeation kinetics of venlafaxine were examined using sheep nasal mucosa mounted onto static vertical Franz diffusion cells. Nasal mucosa was treated with venlafaxine in situ gel (100 ll; 1% w/v) for 7 h. Amount of venlafaxine diffused through mucosa was measured using validated RP-HPLC method. After the completion of the study histopathological investigation of mucosa was carried out. Ex vivo studies through sheep nasal mucosa showed sustained diffusion of venlafaxine with 66.5% permeation in 7 h. Transnasal transport of venlafaxine followed a non-Fickian diffusion process. Permeability coefficient and steady state flux were found to be 21.11 - 10.3 cm h-1 and 21.118 lg cm^2 h^{-1} respectively. Cumulative amount permeated through mucosa at 7 h was found to be 664.8 lg through an area of 3.14 cm2. Total recovery of venlafaxine at the end of the permeation study was 87.3% of initial dose distributed (i) at the mucosal surface (208.4 lg; 20.8%) and (ii) through mucosa (664.8 lg; 66.5%). Histopathological examinations showed no significant adverse effects confirming that the barrier function of nasal mucosa remains unaffected even after treatment with venlafaxine in situ gel. Permeation through sheep nasal mucosa using in situ gel demonstrated a harmless nasal delivery of venlafaxine, providing new dimension to the treatment of chronic depression. This study gives the evidence for nasal transport of Venlafaxine which can be exploited further for the treatment of depression. The nasal route minimizes the risk of systemic adverse events. Histopathology study showed no evidence of any noticeable histological effects, confirming the safety of nasal venlafaxine delivery. Nasal delivery of venlafaxine using mucoadhesive in situ gel is a promising and safe approach for improving the bioavailability and targeting the brain, for the treatment of depression.

3.2 Literature review on nanoparticles

Wang et. al[15] prepared estradiol loaded chitosan nanoparticles using ionic gelation technique and tripolyphosphate anions (TPP) was used as a cation. The prepared nanoparticles had a mean size of 269.3 nm, a zeta potential of +25.4 mV, and loading capacity of estradiol chitosan-NPs suspension was found to be 1.9 mg / ml, % drug entrapment efficiency was 64.7%.The authors proved that the plasma levels obtained following intranasal administration were significantly lower than those after

intravenous administration, while CSF concentrations achieved after intranasal administration were significantly higher than those after intravenous administration. Drug targeting index of nasal route was found to be 3.2 percent and drug targeting (DTP%) was 68.4%. The results revealed that the estradiol must be directly transported from the nasal cavity into the CSF in rats. Further chitosan due to its mucoadhesive character thus increases residual time at the site of administration. They showed that as compared with estradiol inclusion complex, estradiol chitosan-NPs gained higher drug concentration in CSF at each sampling time following intranasal delivery that proved that chitosan-NPs are a more suitable formulation for estradiol to be transported into CNS.

Beduneau et. al[16] prepared nanocarriers loaded with drug that are capable of targetting brain capillary endothelial cells and cerebral tumoral cells and shown promising potential in the field of oncology. Endogenous and chimeric ligands binding to carriers or receptors of the BBB have been directly or indirectly conjugated to nanocarriers. They showed that targeted nanocarriers are a promising tool to deliver drugs and genes to cerebral tumors. Surface-modified nanocarriers were prepared by direct conjugation of site directing ligands or indirectly by the coating of surfactants. This active targeting strategies very effective in the direct transport of drugs to the CNS via nasal cavity. Endogenous and chimeric ligands, including small molecular weight nutrients, proteins and peptides were conjugated directly to nanocarriers using a covalent or a non-covalent linkage. This approach can be widely developed for liposomal systems.

Luppi et. al[17] and team developed chitosan/pectin based nasal inserts to improve bioavailability and therapeutic efficacy of antipsychotic drugs used for the treatment of psychotic symptoms. They prepared polyelectrolyte complexes using different molar pectin/chitosan ratio at pH 5.0 with different polycation/polyanion molar ratios and lyophilized in small inserts in the presence of chlorpromazine hydrochloride. They showed that higher amount of pectin in the complexes, with respect to higher amount of chitosan, produced a more porous structure of the nasal inserts, improving water uptake ability and mucoadhesion capacity. They showed that the presence of increasing amounts of pectin allowed the interaction with chlorpromazine hydrochloride inducing the formation of less hydratable inserts thus limiting drug release and permeation and

thus providing sustained delivery. The results in this study indicated that chitosan/pectin polyelectrolyte complexes can be employed for the formulation of mucoadhesive nasal inserts with different drug release properties.The selection of suitable chitosan/pectin molar ratio during complex preparation allowed the modulation of insert water uptake behaviour and chlorpromazine hydrochloride release and permeation at the administration site.

Abdelbary et. al[18] prepared olanzapine (OZ) nanoparticles, atypical antipsychotic drug that suffers from low brain permeability due to efflux by P-glycoproteins and hepatic first-pass metabolism. This work aimed to develop OZ-loaded micellar nanocarriers and investigate their nose-to-brain targeting potential. Pluronic mixture of L121 and P123 were used to prepare nanoparticles, adopting thin-film hydration method. Spherical micelles ranging in size from 18.97 to 380.70 nm were successfully developed. At a drug:Pluronic® L121:Pluronic® P123 ratio of 1:8:32 (F11), the micelles achieved a conciliation between kinetic and thermodynamic stability, high drug- EE%, controlled drug-release characteristics and evoked minor histopathological changes in sheep nasal mucosa. The significantly ($P < 0.05$) higher values for micelles (i.n.); brain/blood ratio (0.92), drug targeting index (5.20), drug targeting efficiency (520.26%) and direct transport percentage (80.76%) results in the development of a promising non invasive OZ-loaded nose-to-brain delivery system for nasal administration. Kinetically and thermodynamically stable micelles were successfully developed using the thin film hydration method. Optimizing the drug: Pluronic®L121: Pluronic®P123 ratio would encourage the development of stable micelles having high drug loads as well as efficient sustained drug-release characteristics.

Chertok et. al[19] explored the possibility of utilizing iron oxide nanoparticles to be used as a drug delivery vehicle for minimally invasive, MRI monitored magnetic targeting of brain tumors. In vivo effect of magnetic targeting on the extent and selectivity of nanoparticle accumulation in tumors of rats harboring orthotopic 9L-gliosarcomas was quantified with MRI. Animals were intravenously injected with nanoparticles (12 mg Fe/kg) under a magnetic field density of 0 T (control) or 0.4 T (experimental) applied for 30 min. Analysis of images revealed that magnetic targeting induced a 5-fold increase in the total glioma exposure to magnetic nanoparticles over non-targeted tumors (p ¼ 0.005) and a 3.6-fold enhancement in the target selectivity

index of nanoparticle accumulation in glioma over the normal brain (p ¼ 0.025). In conclusion, accumulation of iron oxide nanoparticles in gliosarcomas can be significantly enhanced by developing magnetic targeting and successfully quantified by MR imaging. Hence, these nanoparticles appear to be a promising vehicle for glioma-targeted drug delivery. Results revealed that continued development of magnetic nanoparticle based systems for the delivery of chemotherapeutic agents to brain tumors is warranted. In addition, the ability to monitor magnetic nanoparticle distribution in vivo using clinically translatable MRI methods developed in this study offers a major advantage to non-invasively validate the localization of the drug delivery vehicle at the respective target site.

Gao et. al[20] demonstrated surface engineering of nanoparticles with lectins that opened a novel pathway to improve the brain uptake of agents loaded by biodegradable PEG-PLA nanoparticles following intranasal administration. Ulex europeus agglutinin I (UEA I), specifically binding to l-fucose, which is mainly located within the olfactory epithelium, was selected as a promising targeting ligand and conjugated onto the PEG-PLA nanoparticles surface with an optimized protocol relying on maleimide-mediated covalent binding technique. The in vivo results in rats suggested that UEA I modification at the nanoparticles surface facilitated the absorption of a fluorescent marker-6-coumarin associated with the nanoparticles into the brain following intranasal administration with significant increase in the area under the concentration–time curve (about 1.7 times) in different brain tissues compared with that of coumarin incorporated in the unmodified ones. UEAI-conjugation also resulted in increased brain-targeting efficiency of nanoparticles. Sugar specific inhigition experiments suggested that the interactions between the nasal mucosa and the lectinised nanoparticles were due to the immobilization of carbohydrate-binding pockets on the surface of the nanoparticles. UEA I-modified nanoparticles distribution profiles indicated their higher affinity to the olfactory mucosa than to the respiratory area. Therefore, the nanoparticles modified with UEA I might serve as potential carriers for brain drug delivery, especially for mental therapeutics with multiple biological effects. Lectin surface modification opened a novel pathway to improve the brain uptake of agents loaded by biodegradable PEG-PLA nanoparticles after nasal administration. UEA I, specifically binding to l-fucose, which is largely located in the olfactory

epithelium in the nasal cavity, might serve as a promising targeting ligand for the brain drug delivery system following intranasal administration.

Wen et. al[21] showed that odorranalectin (OL) was recently identified as the smallest lectin with much less immunogenicity than other members of the lectin family. To improve nose-to-brain drug delivery and reduce the immunogenicity of traditional lectin modified delivery system,OL was conjugated to poly(ethylene glycol)–poly(lactic-co-glycolic acid) (PEG–PLGA) nanoparticles and its biorecognitive activity on nanoparticles was verified by haemagglutination tests. Nose-to-brain delivery characteristic of OL-conjugated nanoparticles (OL-NP) was investigated by in vivo fluorescence imaging technique using DiR as a tracer. Besides, urocortin peptide (UCN), as a model drug, was incorporated into nanoparticles and evaluated for its therapeutic efficacy on hemiparkinsonian rats following intranasal administration by rotation behavior test, neurotransmitter determination and tyrosine hydroxylase (TH) test. The results suggested that OL modification increased the brain delivery of nanoparticles and enhanced the therapeutic effects of UCN loaded nanoparticles on Parkinson's disease. The OL-NPs could be potentially used as carriers for nose-to-brain drug delivery, especially for macromolecular drugs, in the treatment of CNS disorders. A novel nose-to-brain delivery system, odorranalectin (OL) conjugated poly(ethylene glycol)–poly(lactic-co-glycolic acid) (PEG–PLGA) nanoparticle, was established in this study. The resulting nanoparticles effectively increased the brain uptake of DiR loaded nanoparticles and enhanced the neuroprotective effects of urocortin (UCN) peptide on hemiparkinsonian rats following intranasal delivery.

Opanasopit et. al[22] studied to investigate the possibility of using pectinate micro/nanoparticles as gene delivery systems. Micro/nanoparticles using pectin were produced by ionotropic gelation. Various factors that influences formulation characteristics were studied by them to determine the effects on the preparation of pectinate micro/nanoparticles: the pH of the pectin solution, the ratio of pectin to the cation, the concentration of pectin and the cation, and the type of cation (calcium ions, magnesium ions and manganese ions). The size and charge of the pectin micro/nanoparticles and their DNA incorporation efficiency were evaluated. The results revealed that the particle sizes decreased with the decreased concentrations of pectin and cation. The type of cations affected the particle size. Sizes of calcium

pectinate particles were larger than those of magnesium pectinate and manganese pectinate particles. The transfection efficiency of both Ca-pectinate and Mg-pectinate nanoparticles yielded relatively low levels of green fluorescent protein expression and low cytotoxicity in Huh7 cells. Given the negligible cytotoxic effects, these micro/nanoparticles can be considered as potential candidates for use as safe gene delivery carriers. The concentration of both pectin and divalent cations (Ca2+, Mg2+ and Mn2+) affected the particle size and shape of pectinate micro/nanoparticles. The DNA-loaded Ca-pectinate and Mgpectinate nanoparticles had the ability to transfect Huh7 cells with low cytotoxicity. This study suggests these pectinate nanoparticles have a potential use as safe gene delivery vectors.

Nagavarma et. al[23] reviewed on polymeric nanoparticles (PNPs) that can be defined as particulate dispersions or solid particles with size rang 10-ing from 10-1000nm. There has been a considerable research interest in the area of drug delivery using particulate delivery systems as carriers for small and large molecules. Particulate systems like nanoparticles have been used as a physical approach to modify and improve the pharmacokinetic and pharmacodynamic properties of various types of drug molecules. Polymeric nanoparticles have been extensively studied as particulate carriers in the pharmaceutical and medical fields, as they show promising drug delivery systems as a result of their controlled and sustained release properties, subcellular size, biocompatibility with tissue and cells. Various methods to have been developed to prepare polymeric nanoparticles and these techniques are classified according to whether the particle formation involves a polymerization reaction or nanoparticles form directly from a macromolecule or preformed polymer. In this review various techniques that can be used for the preparation of polymeric nanoparticles are described. The main goal of this review was to describe the different preparation techniques available for production of polymeric nanoparticles. The drug-loaded nanospheres or nanocapsules now can be produced by simple, safe, and reproducible techniques available. Depending on the physicochemical characteristics of a drug, it is possible to choose the best method of preparation and the polymer to produce nanoparticles with desired size range with good entrapment efficiency of the drug. The limitations like one particular process or technique is not suitable to all drugs, post preparative steps, such as purification and preservation, incomplete or discontinuous film, inadequate stability of certain active components are remained to solve. Despite

these technological challenges, nanoparticles have been showed great promise for the development of drug delivery system.

3.3 Literature review on intranasal insitu gel

Vyas et. al[24] prepared sumatriptan (ST) and sumatriptan succinate (SS) containing microemulsion to accomplish rapid delivery of drug to the brain in case of acute migraine attacks and carried out in vivo evaluation in rats. Sumatriptan microemulsions (SME)/sumatriptan succinate microemulsions (SSME) were prepared using titration method and characterized for globule size, drug content, size distribution, and zeta potential. Biodistribution study of SME, SSME, sumatriptan solution (SSS), and marketed product (SMP) in the brain and blood of Swiss albino rats following intranasal and intravenous (IV) administrations were examined using optimized technetium labeled (99mTc-labeled) ST formulations. Various pharmacokinetic parameters like drug targeting efficiency (DTE), and direct drug transport (DTP) were derived by them. Gamma scintigraphy imaging of rat brain following IV and intranasal administrations were performed to ascertain the localization of drug in CNS. SME and SSME were transparent and stable with mean globule size 38 ± 20 nm and zeta potential between −35 to −55 mV. Results of brain/blood uptake ratios at 0.5 hour following IV administration of SME and intranasal administrations of SME, SMME, and SSS were 0.20, 0.50, 0.60, and 0.26, respectively, suggesting effective transport of drug to the CNS following intranasal administration of microemulsions. Higher DTE and DTP for mucoadhesive microemulsions indicated more effective targeting following intranasal administration and best brain targeting of ST from mucoadhesive microemulsions. They demonstrated rapid and higher extent of transport of drug from microemulsion of ST compared with microemulsion of SS, SMP, and SSS into the rat brain. Hence, intranasal delivery of ST microemulsion developed in this investigation can play a promising role in the treatment of acute attacks of migraine. The studies demonstrated rapid and larger extent of selective ST nose-to-brain transport compared with SS and SMP in rats. Enhanced rate of transport of ST following intranasal administration of SMME may result in decreasing the dose and frequency of dosing and possibly maximize the therapeutic index. However, clinical benefits to the risk ratio of the formulation developed in this investigation will decide its appropriateness in the clinical practice.

Qian et. al[25] aimed to develop an in situ gel formulation tacrine (THA), for intranasal delivery of an anti-Alzheimer's drug. Thermosensitive polymer Pluronic F-127 was used to prepare THA in situ gels. Sol–gel transition temperature (Tsol–gel), rheological properties, in vitro release and in vivo nasal mucociliary transport time were optimized. Pharmacokinetics and brain dispositions of in situ gel were compared with that from THA oral solution in rats. The formulated in situ gel demonstrated a liquid state with Newtonian fluid behavior under 20^{o}C, while it exhibited as non-flowing gel with pseudoplastic fluid behavior beyond its Tsol–gel of 28.5^{o}C. Based on nasal mucociliary transport time, the in situ gel containing mucoadhesive agent significantly prolonged its retention in nasal cavity compared to its solution form. The in situ gel achieved 2–3 fold higher peak plasma concentration (Cmax) and area under the curve (AUC) of THA in plasma and brain tissue,but lowered Cmax and AUC of the THA metabolites compared to that of oral solution. The enhanced nasal residence time due to its mucoadhesive nature improved bioavailability, increased brain uptake of parent drug and decreased exposure of metabolites suggested that the in situ gel could be an effective intranasal formulation for THA. Pluronic F-127 based thermo- sensitive in situ gel of THA with favorable physiochemical properties (suitable Tsol–gel,rheological properties and slow release kinetics) was developed. The enhanced residence time in nasal cavity, improved bioavailability and brain uptake of THA suggested that in situ gel could serve as an intranasal formulation for THA.

Patel et. al[26] developed nasal mucoadhesive gel of Glimepiride for controlled release. Carbopol 934p was used as a key ingredient which gives mucoadhesion property to the gel formulations. Different formulations were prepared by varying the concentrations of Carbopol 934p and Hydroxyl Propyl Methyl Cellulose K4M (HPMC K4M). These formulations were evaluated for parameters like pH, Drug content, Viscosity, Mucoadhesive strength, Gel strength, In-vitro drug release, In-vitro permeation and Drug excipient compatibility. In this formulation the release profile depend on the concentration of Carbopol 934p and HPMC K4M. A 32 factorial design was applied to see the effect of variables Carbopol 934p (X1) and HPMC K4M (X2) on the response percentage drug release as a dependent variable. In vitro release data were fitted to various models to ascertain kinetic of drug release. Regression analysis and analysis of variance were performed for dependent variables. The results of the F-statistics were used to select the most appropriate model. Formulation containing Carbopol 934p(1.0%) and HPMC K4M(1.0%) was found to be optimum.

Ved et. al[27] investigated the olfactory transfer of zidovudine (ZDV) after intranasal (IN) administration and assessed the effect of thermoreversible gelling system on its absorption and brain uptake. The nasal formulation was prepared by dissolving ZDV in pH 5.5 phosphate buffer solution comprising of 20% polyethylene oxide/propylene oxide (Poloxamer 407, PLX) as thermoreversible gelling agent and 0.1% n-tridecyl-d-maltoside (TDM) as permeation enhancer. This formulation exhibited a sufficient stability and an optimum gelation profile at 27–30 ◦C. The in vitro permeation studies across the freshly excised rabbit nasal mucosa showed a 53% increase in the permeability of ZDV from the formulation. For in vivo evaluation, the drug concentrations in the plasma, cerebrospinal fluid (CSF) and six different regions of the brain tissues, i.e. olfactory bulb, olfactory tract, anterior, middle and posterior segments of cerebrum, and cerebellum were determined by LC/MS method following IV and IN administration in rabbits at a dose of 1 mg/kg. The IN administration of Poloxamer 407 and TDM based formulation showed a systemic bioavailability of 29.4% while exhibiting a 4 times slower absorption process (tmax = 20 min) than control solution (tmax = 5 min). The CSF and brain ZDV levels achieved after IN administration of the gelling formulation were approximately 4.7–56 times greater than those attained after IV injection. The pharmacokinetic and brain distribution studies revealed that a polar antiviral compound, ZDV could preferentially transfer into the CSF and brain tissue via an alternative pathway, possibly olfactory route after intranasal administration. The in vivo absorption and brain distribution studies in rabbits revealed that a polar antiviral agent, zidovudine could preferentially transfer into the cerebrospinal fluid and brain tissues from the nasal cavity possibly via olfactory pathway. Intranasal administration of ZDV solution formulated with a thermo-reversible gelling system prepared with Poloxamer 407 in aqueous buffer solution containing n-tridecyl-d-maltoside as permeation enhancer may provide a promising and durable therapeutic option for the treatment of CNS disorders caused by human immunodeficiency virus.

Saindane et. al[28] developod in situ gelling nasal spray formulation of carvedilol (CRV) nanosuspension to improve the bioavailability and therapeutic efficiency. Solvent precipitation–ultrasonication method was opted for the preparation of CRV nanosuspension which further incorporated into the in situ gelling polymer phase.

Optimized formulation was extensively characterized for various physical parameters like in situ gelation, rheological properties and in vitro drug release. Formation of in situ gel upon contact with nasal fluid was conferred via the use of ion-activated gellan gum as carrier. In vivo studies in rabbits were performed comparing the nasal bioavailability of, CRV after oral, nasal, and intravenous administration. Optimized CRV nanosuspension prepared by combination of poloxamer 407 and oleic acid showed good particle size [d (0.9); 0.19 μm], zeta potential (+10.2 mV) and polydispersity (span; 0.63). The formulation containing 0.5%w/v gellan gum demonstrated good gelation ability and desired sustained drug release over period of 12 h. In vivo pharmacokinetic study revealed that the absolute bioavailability of in situ nasal spray formulation (69.38%) was significantly increased as compared to orally administered CRV (25.96%) with mean residence time 8.65 h. Hence, such in situ gel system containing drug nanosuspension is a promising approach for the intranasal delivery in order to increase nasal mucosal permeability and in vivo residence time which altogether improves drug bioavailability.

4 Materials and Methods

4.1 Materials:

Table 4.1: List of Materials used

Materials	Company Name
Venlafaxine hydrochloride	Cadila Healthcare Ltd., Ahmedabad, India
Pectin	Triveni Chemicals, Baroda, India
Magnesium Chloride	Triveni Chemicals, Baroda, India
Calcium Chloride	Triveni Chemicals, Baroda, India
Zinc Chloride	Triveni Chemicals, Baroda, India
Poloxamer 188	Cadila Healthcare Ltd., Ahmedabad, India
Poloxamer 477	Cadila Healthcare Ltd., Ahmedabad, India
HPMC K4M	Triveni Chemicals, Baroda, India
Carbool 934 P	Triveni Chemicals, Baroda, India
Stearic acid	Triveni Chemicals, Baroda, India
Hydrochloric acid AR	Triveni Chemicals, Baroda, India
Sodium hydroxide	Triveni Chemicals, Baroda, India
Distilled water	Prepared in lab

4.2 Methods

4.2.1 Identification of Venlafaxine hydrochloride

A) Melting Point Determination: [13]

Melting point is the temperature at which the pure liquid and solid exist in the equilibrium. In the practice it is taken as equilibrium mixture at an external pressure of 1 atmosphere. The thiel's tube method of melting point determination in liquid paraffin was used in the present study. Melting point was found to be 214°C-216°.

Table 4.2: Melting point determination

Melting Point	Standard value	Observed Value
	213-216°C	214°C-216°C

Conclusion: The melting point determined was within the range of standard value, hence, it was concluded that the drug sample having intimate physical property as standard drug.

B) Determination by UV spectroscopy: [13]

UV scanning was done for 10 µg/ml drug solution from 200-400 nm in Phosphate buffer pH 6.4 as a blank using Shimadzu UV 1800 double beam UV/Visible spectrophotometer. The absorption maxima was found to be at 226 nm.

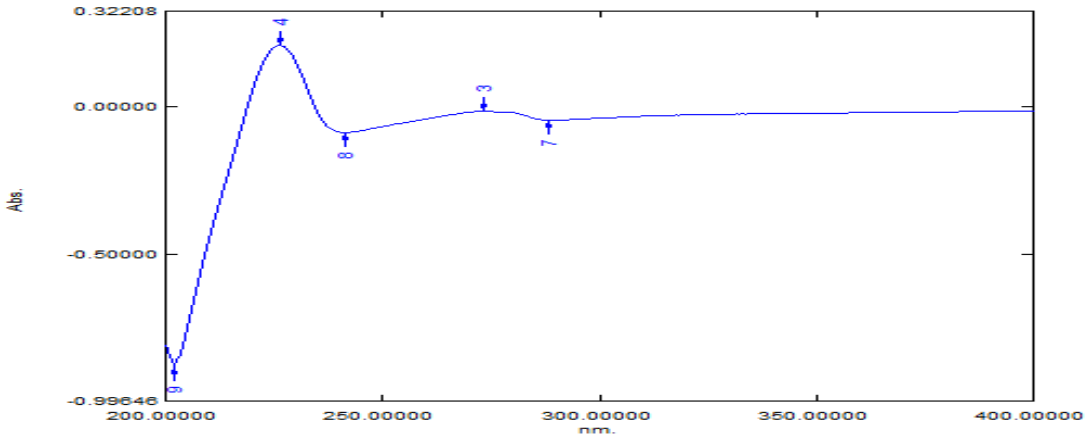

Figure 4.1: UV absorbance spectra of Venlafaxine hydrochloride Phosphate buffer 6.4

Table 4.3: Determination of λ_{max}

Concentration	λ_{max} (nm)	Absorbance
16 µg/ml	226 nm	0.215

Conclusion: The above UV spectra of Venlafaxine HCl showed the λmax at 226 nm, which was constant after dilution and in range to the reported standard value (224) nm. This also indicated identity and purity of the drug sample.

C) Determination by IR Spectra (FTIR): [13]

FTIR spectra of drug in KBR pellets at moderate scanning speed between 4000-400 cm-1 was carried out using FTIR (Jasco FTIR 6100 TYPE A, Japan). All the powder

samples were dried under vacuum prior to obtaining any spectra in order to remove the influence of residual moisture.

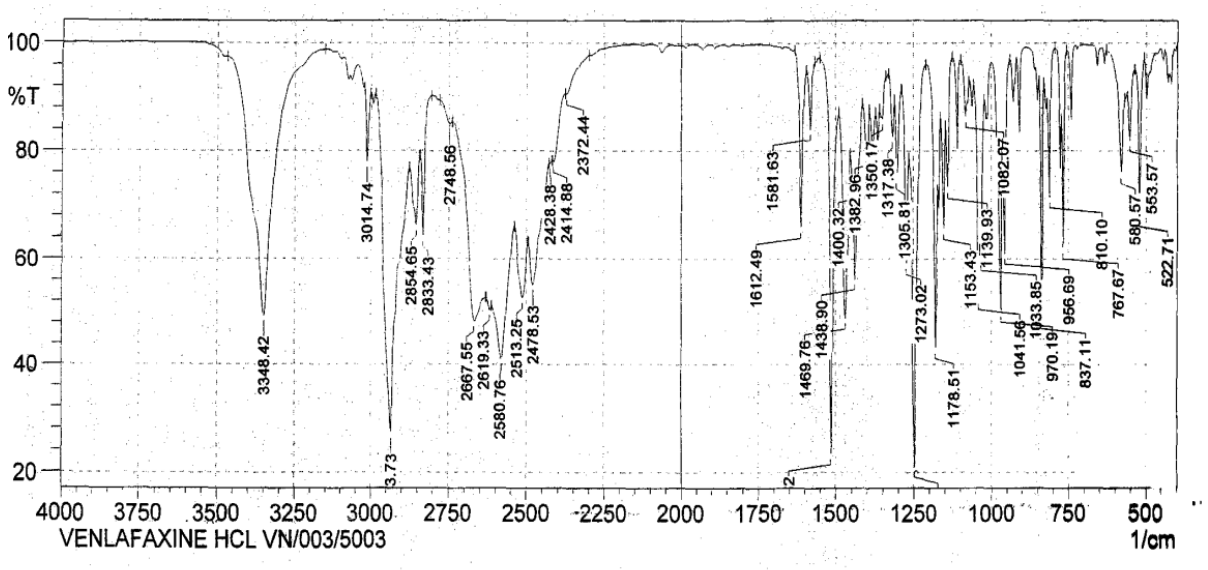

Figure 4.2: Reference FTIR spectra of Venlafaxine hydrochloride

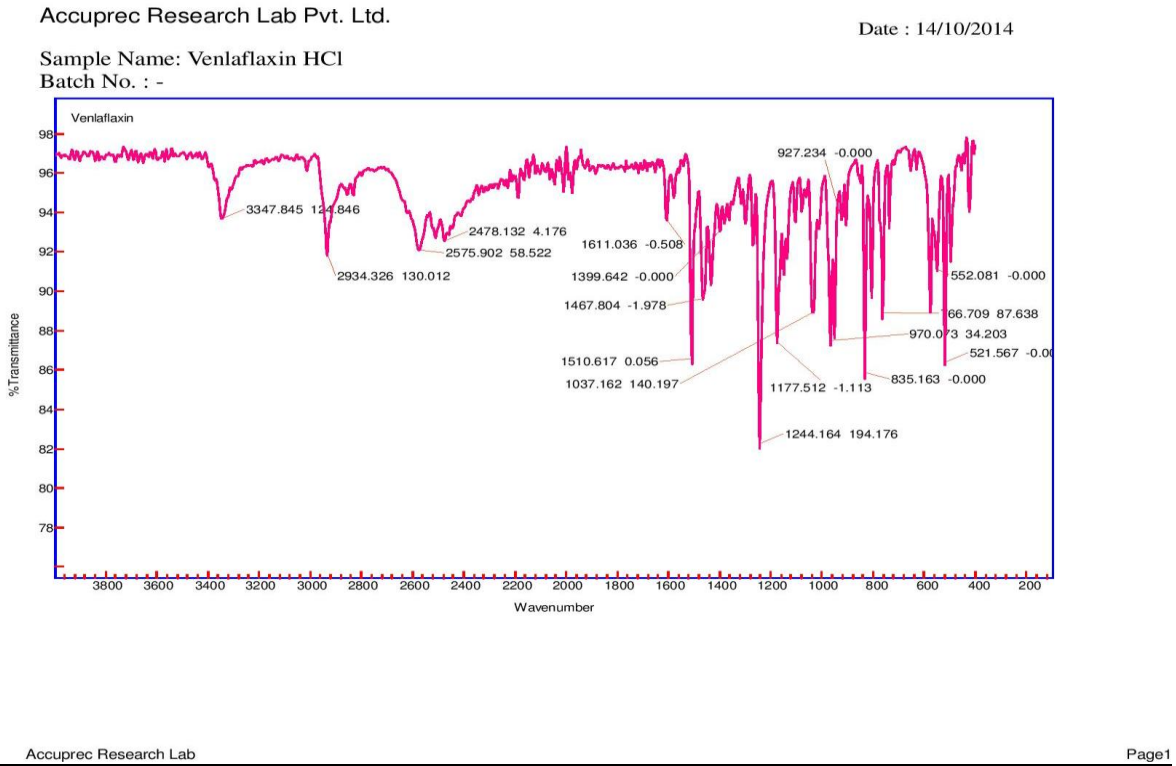

Figure 4.3: Observed FTIR spectra of Venlafaxine hydrochloride

Table 4.4: FTIR interpretation of venlafaxine hydrochloride

Sr.No	Functional group	Standard frequency (cm^{-1})	Observed frequency

			(cm^{-1})
1	OH	3300-3400	3347.84
2	C6H5	1500-1600	1467.80
3	Aliphatic CH	2800-3000	2934.32
4	C-O-C	1000-1200	1177.51

Discussion: The sample spectrum of Venlafaaxine hydrochloride was compared with standard one and both spectra were found similar in peak values representing wave numbers. Thus, it can be concluded that procured Venlafaxine hydrochloride sample was a pure drug.

D) Establishment of calibration curve of Venlafaxine hydrochloride in Phosphate buffer (pH 6.4):

Preparation of stock solution:

10 mg of Venlafaxine hydrochloride was accurately weighed and transferred into 100 ml volumetric flask. It was dissolved in phosphate buffer (pH 6.4) and volume was made up to the mark with phosphate buffer (pH 6.4) to get 100 µg/ml solution.

Preparation of Standard Curve:

A primary stock solution was prepared by weighing accurately 100 mg of Venlafaxine hydrochloride on an analytical balance. The drug was transferred into 100 ml volumetric flask and then 25 ml of phosphate buffer (pH 6.4) was added and sonicated for 15 mins. The final volume was made up to 100 ml with phosphate buffer (pH 6.4) and was mixed well. A series of dilutions were prepared by withdrawing required amount of volume like 0.5, 1.0, 1.5, 2.0, 2.5, 3.0, 3.5 ml from stock solution (100 µg/ml) and were transferred to a 10 ml volumetric flask. The final volume was made up to 10 ml with phosphate buffer (pH 6.4) to get concentration in the range of 0-35 µg/ml respectively.

Table 4.5: Standard curve of venlafaxine hydrochloride in phosphate buffer (ph 6.4)

Concentration (µg/ml)	Absorbance 1	Absorbance 2	Absorbance 3	Average Absorbance

0	0	0	0	0
5	0.132	0.131	0.133	0.132
10	0.231	0.233	0.229	0.166
15	0.426	0.429	0.423	0.193
20	0.635	0.631	0.639	0.210
25	0.783	0.781	0.785	0.226
30	0.864	0.862	0.866	0.253
35	0.964	0.967	0.961	0.289

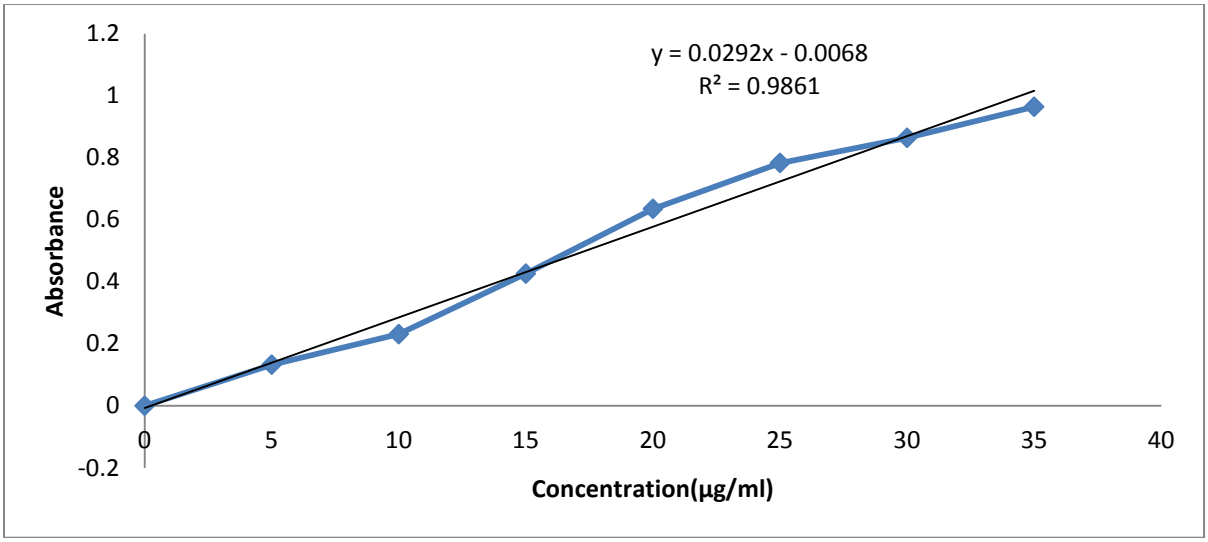

Figure 4.4: Standard curve of Venlafaxine hydrochloride in phosphate buffer (pH 6.4)

Table 4.6: Regression analysis for standard curve of Venlafaxine hydrochloride in phosphate buffer (pH 6.4)

Regression parameter	Value
Correlation coefficient	0.986
Slope	0.006
Intercept	0.029

4.2.2 Drug Excipient compatibility study: [13]

Compatibility studies were performed using FT-IR spectroscopy, the IR Spectra of pure drug and physical mixture of Drug and Polymer were studied by making a KBr mixture. The characteristic absorption peaks of Venlafaxine HCl were obtained at different wave number in different sample. The peak obtained in the formulation

spectra correlates with the peaks of drug spectra. This indicates that the drug is compatible with the formulation component. The spectra for all formulation shown below.

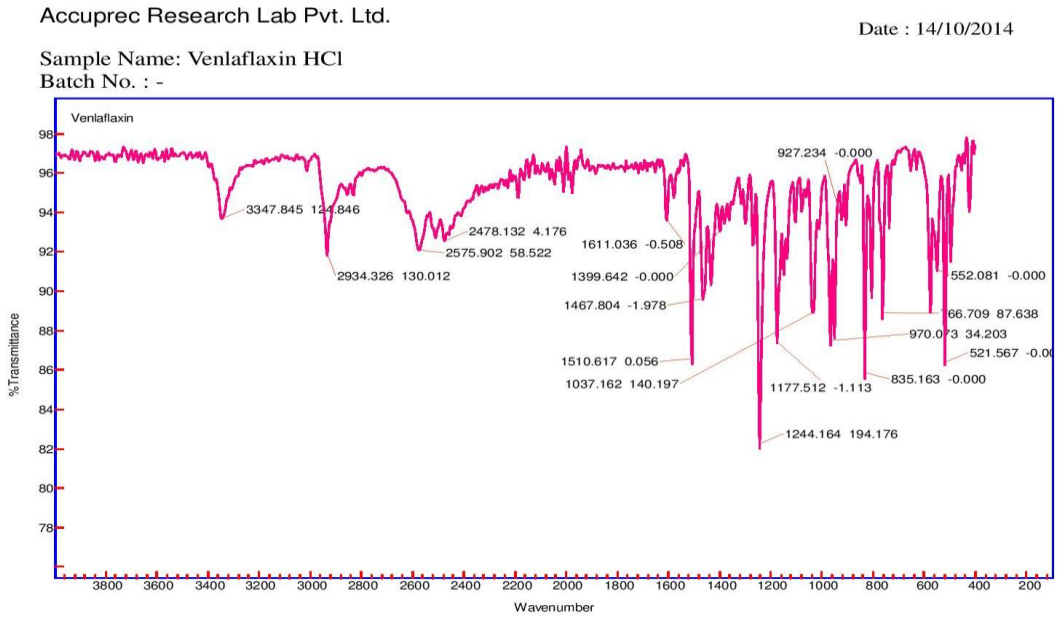

Fig. 4.5: Observed FTIR spectra of Venlafaxine HCl

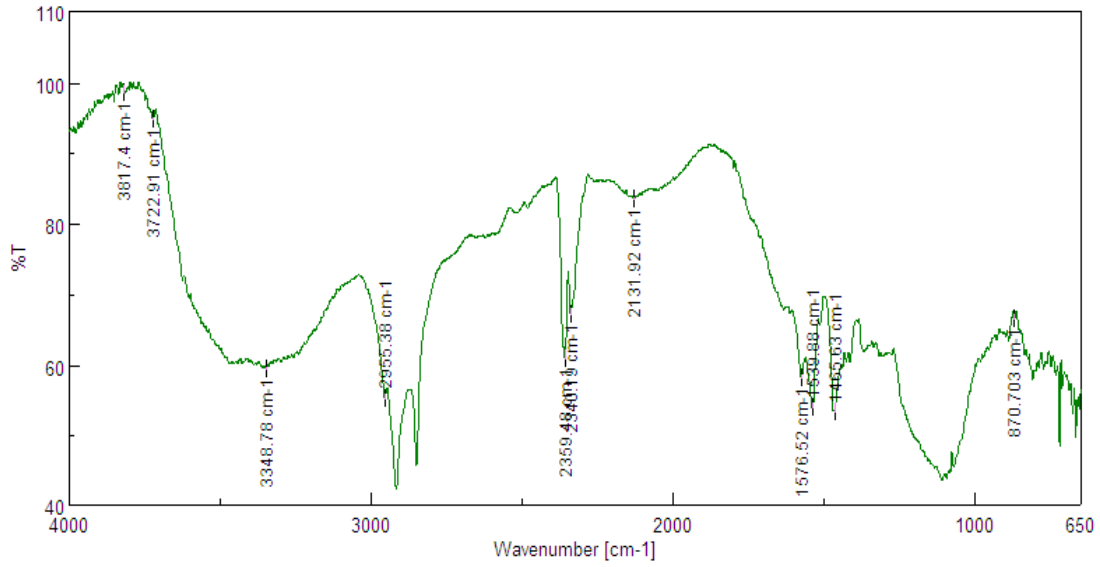

Fig. 4.6: Observed FTIR spectra of Excipients blend

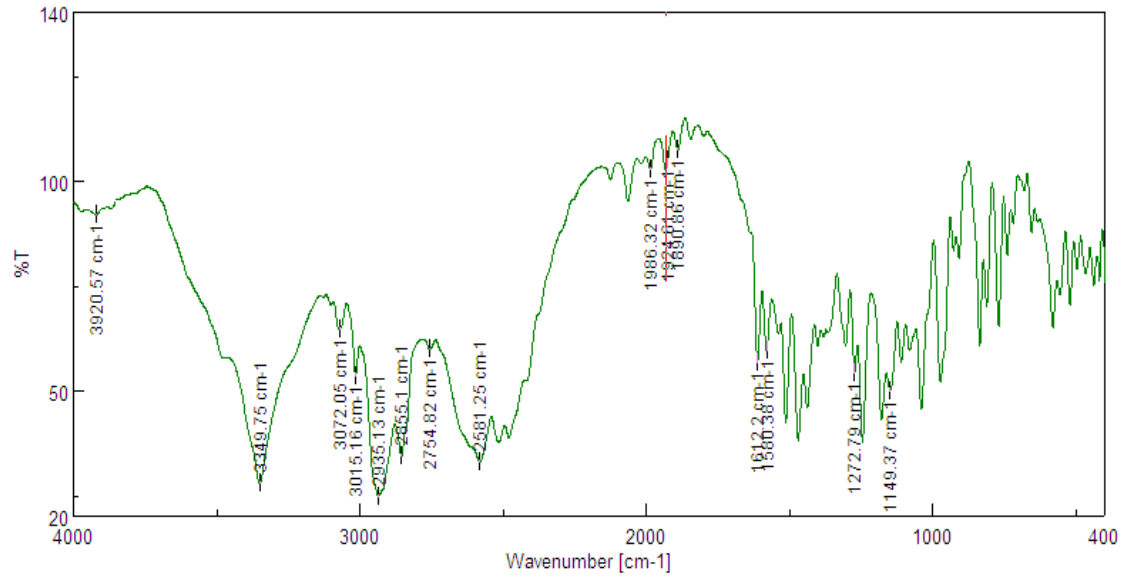

Figure 4.7: Observed FTIR spectra of Drug Excipients blend

Table 4.7: Comparison of Drug and Drug Excipient blend IR frequency

Functional group	Standard frequency (cm^{-1})	Observed frequency (cm-1)
Aromatic (C-H str.)	3000-3100	3008.41
N-H stretching	3300-3350	3349.75
C-O stretching	1020-1150	1038.45
CH_2 (C-H Str.)	2850-2950	2940.91

Conclusion: Compatibility studies for the drug and excipients were conducted using FT-IR spectrophotometer. Venlafaxine and various polymer mixtures showed their respective characteristic bands. The Venlafaxine HCl-excipient blend retained all the characteristic peaks of Venlafaxine HCl& hence it was confirm that there was no chemical interaction between drug and excipients.

4.3 Preparation of Nanoparticulate suspension

4.3.1 Preparation of Nanoparticles: [22]

Nanoparticles were prepared by ionic gelation technique.Briefly, pectin was dissolved in distilled water to a concentration ranging from 0.5-1%. The divalent cation ($MgCl_2$, $CaCl_2$, $ZnCl_2$) was dissolved in distilled water in a concentration ranging from 0.25-1%. Nanoparticles were prepared by drop-wise addition of pectin solution to a divalent cation ($MgCl_2$, $CaCl_2$, $ZnCl_2$) solution while the solution was constantly stirred at 25^0C. Stirring was further continued for another 30 minutes and nanoparticles were separated by centrifuging at 8000 rpm for about 3 hours for particle size determination.

4.3.2 Preparation of insitu gelling polymeric phase: [28]

Solution of Poloxamer 407 in concentration range of 15-30 % were prepared by dissolving it in distilled water. This solution was cooled overnight for complete dissolution of poloxamer 407 til clear solution is obtained. To this appropriate concentration of HPMC K4M (0.1-0.7%) was dissolved with constant stirring. The solution was further cooled for an hour to obtain clear solution and was stored at cool temperature.

4.3.3 Preparation of insitu gelling nanosuspension of venlafaxine hydrochloride:

Prepared nanoparticles were suspended in the insitu gelling polymeric phase and was stirred for 20 minutes for uniform distribution.To this nanosuspension 1% stearic acid and 1% carbopol 934P were incorporated as a stabilizer and mucoadhesive agent respectively.

4.4 Invitro Characterization of Venlafaxine hydrochloride nanoparticles

4.4.1 Particle Size and Zeta-Potential Measurements: [22]

The mean particle size and zeta potential of the venlafaxine hydrochloride loaded pectinate nanoparticles were determined in triplicate at 25°C by photon correlation spectroscopy (PCS) using the Zetasizer Nano ZS (Malvern Instruments, Malvern, UK). The pectinate nanoparticulate samples were diluted with distilled water that had been filtered through a 0.22-μm membrane filter.

4.4.2 Morphology: [22]

The morphology of the venlafaxine hydrochloride loaded pectinate nanoparticles was investigated by transmission electron micrograph. Briefly, three percentage solution of formvar was prepared in spectroscopic-grade chloroform. Then, one drop of pectinate nanoparticulate sample solution was put on a formvar-coated carbon ultra-thin grid and air dried. The dried grid was then examined under scanning electron microscope.

4.4.3 Drug Entrapment Efficiency: [22]

The drug association capacity of the nanoparticles was evaluated after separation of the nanoparticles by centrifugation of the nanoparticle suspension at 8,000 rpm for 30 min. The amount of free drug in the supernatant was determined in triplicate by UV spectrophotometer (λmax 236 nm). The drug association capacity was calculated using following equation:

The percent association capacity = 100*Total drug incorporated – Free drug in supernant

---

Total drug incorporated

4.4.4 In Situ Gelling Ability and Viscosity Determination: [28]

The viscosity of the insitu gelling polymeric formulation con0taining different concentrations of poloxamer (15%, 20%, 25% and 30 %w/v) was determined with and without artificial nasal fluid on rotational viscometer (Brookfield Viscometer). Measurements were performed using suitable spindle number at 50 rpm at 37°C. In situ gelling ability of optimized formulation was demonstrated by mixing formulation and artificial nasal fluid (1:1v/v) in a glass vial and gelation was observed by visual examination after inverting the vial. An in situ gelation of formulation was demonstrated by spraying formulation on filter paper soaked with simulated nasal fluid.

4.4.5 In Vitro Drug Release in Simulated Nasal Fluid:[22,28]

In vitro drug release study of nanoparticles was performed using USP paddle apparatus.A dialysis tube (dialysis membrane-70; molecular weight cutoff: 12,000, Himedia, India) containing 2.0-ml formulation was immersed in 200 ml of simulated nasal electrolyte solution (7.45 mg/ml NaCl, 1.29 mg/ml KCl, and 0.32 mg/ml $CaCl_2 \cdot 2H2O$ and pH adjusted at 6.4) used as a dissolution medium at 34±0.5°C and at peddle speed of 50 rpm. The amount of drug released from the formulation was measured spectrophotometrically at λmax 226 nm. The concentration of drug was determined from a previously constructed calibration curve.

5.1 Formulation of pectinate nanoparticles by ionic gelation method: [30]

Ionotropic gelation technique is based on the ability of polyelectrolytes to cross link in the presence of counter ions to form hydrogel beads also called as gelispheres. Gelispheres are spherical crosslinked hydrophilic polymeric entity that are capable of extensive gelation and swelling in the presence of simulated biological fluids and the release of drug through it is controlled by polymer relaxation. The hydrogel beads are produced by dropping a drug-loaded polymeric solution into the aqueous solution of polyvalent cations with continuous stirring.The cations diffuses into the drug-loaded polymeric drops, forming a three dimensional lattice of ionically crosslinked moiety. Biomolecules can also be loaded into these gelispheres under mild conditions to retain their three dimensional structure.

Table No 5.1: Various polymers and cations used for the preparation of nanoparticles

Natural polymers	Synthetic monomers/polymers	Multivalent Cations
Chitosan Alginate Fibrin Collagen Gelatin Hyaluronic acid Dextran	Hydroxyethyl methacryate (HEMA) N-(2-Hydroxypropyl) methacrylate (HPMA) N-Vinyl-2-pyrrolidone (NVP) N-Isopropylacrylamide (NIPAMM) Vinyl acetate (VAc) Acryolic acid (AA) Methacrylic acid (MAA)	Calcium (Ca^{+2}) Potassium (K^{+}) Ferric (Fe^{+2}) Barium (BA^{+2}) Sodium (Na^{+}) Magnesium (Mg^{+2}) Aluminium (Al^{+3}) Zinc (Zn^{+2})

	Polyethylene glycol acrylate/methacrylate (PEGA/PEGMA) Polyethylene glycol diacrylate/dimethacrylate (PEGDA/PEGDMA)	

5.1.1 Preliminary trials

5.1.1.1 Effect of different parameters:

A.Pectin:Divalent cation concentration ratio:

Batches PM1-PM4, PC1-PC4, PZ1-PZ4 were prepared by using different ratios of pectin to divalent cation ($MgCl_2$, $CaCl_2$, $ZnCl_2$) respectively. Various batches reveal the effect of pectin to cation ratio on particle size, zeta potential, % drug entrapment efficiency and % drug released.

Table No 5.2:- Composition of batches PM1-PM4

Batch No.	Concentration of Pectin	Concentration of $MgCl_2$
PM1	0.5	0.5
PM2	0.5	1
PM3	1	0.5
PM4	1	1

Table No 5.3:- Composition of batches PC1-PC4

Batch No.	Concentration of Pectin	Concentration of $CaCl_2$
PC1	0.5	0.5
PC2	0.5	1
PC3	1	0.5
PC4	1	1

Table No 5.4:- Composition of batches PZ1-PZ4

Batch No.	Concentration of Pectin	Concentration of $ZnCl_2$
PZ1	0.5	0.5

PZ2	0.5	1
PZ3	1	0.5
PZ4	1	1

Results of various batches on particle size, zeta potential, % drug entrapment efficiency and % drug released after 24 hours are as follows

Table No 5.5:- Results of particle size analysis, zeta potential, % entrapment efficiency, % drug released

Batch No	Mean particle size (nm)	Zeta Potential (mV)	% Entrappment Efficiency	% Drug released after 24 hours
PM1	509.4	-20.4	70.6%	86.44
PM2	536.2	-22.6	71.4%	81.30
PM3	812.5	-24.6	74.6%	78.62
PM4	990.8	-26.4	75.1%	72.18
PC1	660.6	-18.4	68.4%	81.35
PC2	890.6	-17.6	69.4%	79.45
PC3	890.6	-19.4	71.5%	76.34
PC4	1100.8	-22.5	73.6%	66.36
PZ1	630.8	-18.4	64.2%	-
PZ2	670.8	-17.6	65.3%	-
PZ3	1180.6	-19.6	69.4%	-
PZ4	1500.6	-22.5	73.1%	-

In Vitro drug release in Simulated Nasal Fluid: [19]

In vitro drug release study of prepared nanoparticles was performed using USP paddle method. A dialysis tube (dialysis membrane; molecular weight cutoff: 12,000, Himedia, India) containing 2.0-ml formulation was immersed in 500 ml of simulated nasal electrolyte solution (7.45 mg/ml NaCl, 1.29 mg/ml KCl, and 0.32 mg/ml $CaCl2{\cdot}2H_2O$ and pH adjusted at 5.5) used as a dissolution medium at 37±0.5°C and at paddle speed of 50 rpm. The amount of drug released from the formulation was measured spectrophotometrically at λ_{max} 226 nm. The concentration of drug was determined from a previously constructed calibration curve.

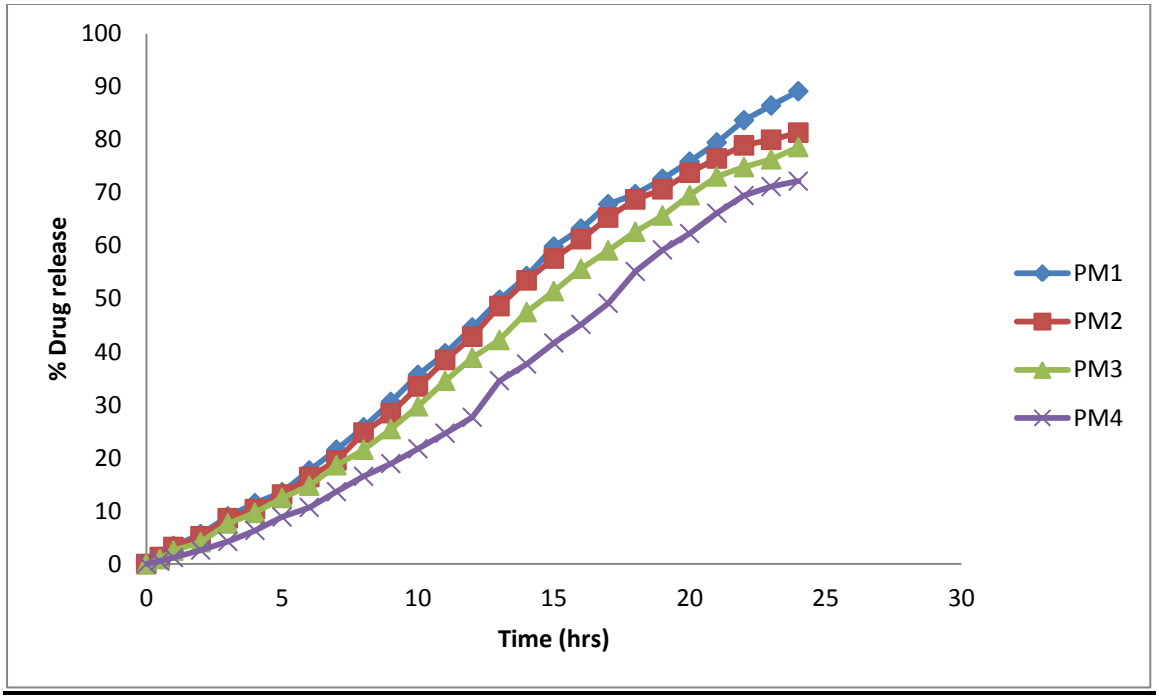

Figure 5.1: Drug release profile for batches PM1-PM4

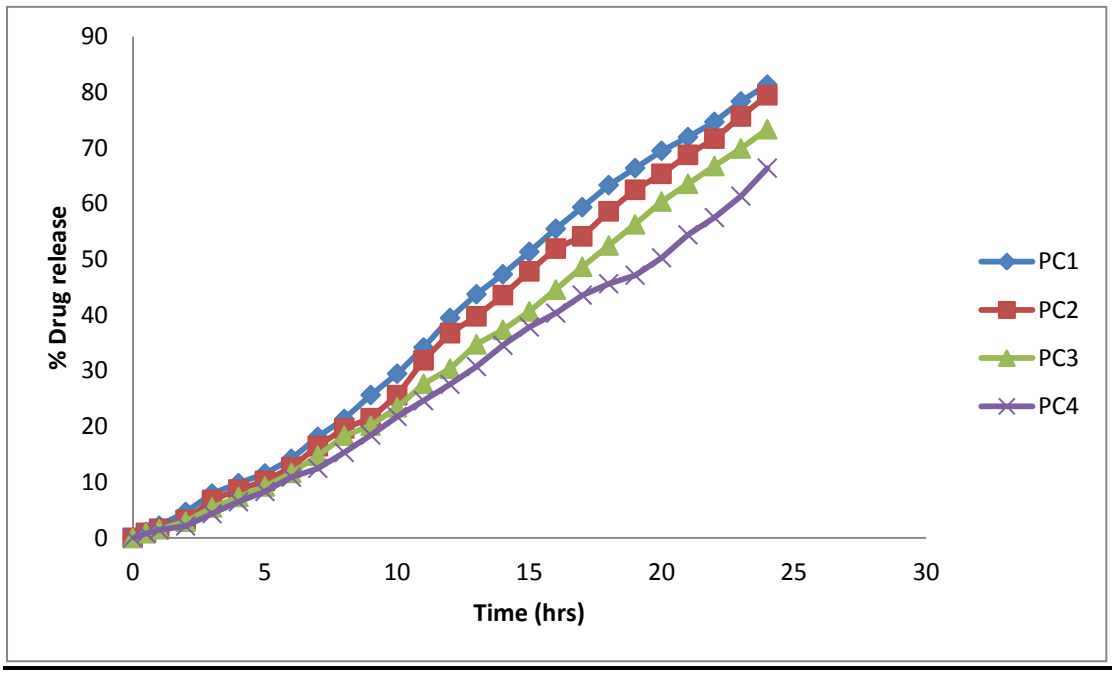

Figure 5.2: Drug release profile for batches PC1-PC4

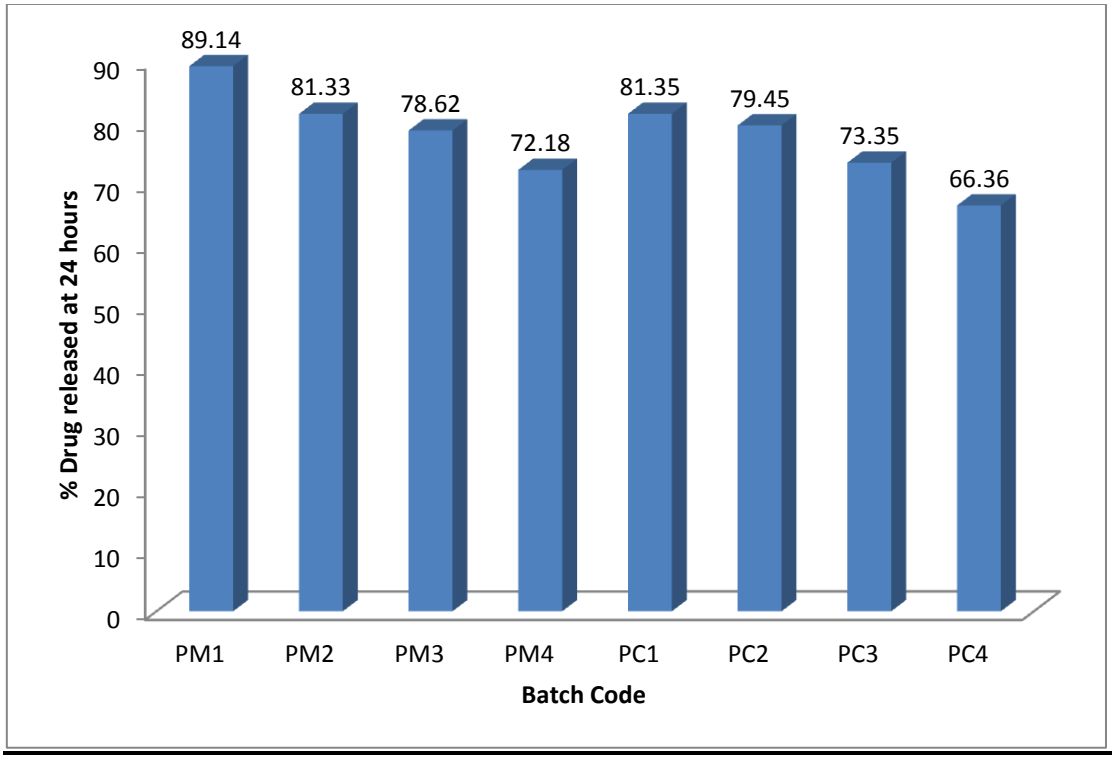

Figure 5.3: Drug released after 24 hours for batches PM1-PM4 & PC1-PC4

Discussion:

Intermolecular cross-linked nanoparticles were formed between the negatively charged carboxyl groups of pectin and the positively charged divalent cations. Preliminary trials showed that gelation of pectin were induced by adding divalent cations ($MgCl_2$, $CaCl_2$ and $ZnCl_2$).

Different batches using pectin in concentration of 0.5% and 1% with $MgCl_2$, $CaCl_2$ and $ZnCl_2$ in concentration range of 0.5% and 1% were prepared and analysed for particle size, zeta potential, % drug entrapmrnt efficiency and % drug released.

Results of particle size reveals that increase in the concentration of divalent cation does not significantly results in increase in the particle size but increase in pectin concentration significantly results in the increase in the particle size as shown in table 5.5. The increase in particle size with increase in pectin concentration is increase in globule size with increase in polymer concentration. As shown in table 5.5 with the pectin solution at a lower concentration, smaller particles were formed in all systems regardless of divalent cation used.

Nanoparticles prepared using Mg^{+2} were smaller in size than Ca^{+2} and Zn^{+2} (when formulated using the same amount and ratio of pectin/ divalent cations). Minimum particle size was achieved with 0.5% concentration of pectin and 0.5% of $MgCl_2$.

Results of zeta potential reveals that increase in the concentration of pectin and results in increase in the negative zeta potential as shown in table 5.5. The increase in zeta potential with increase in pectin concentration is due to increase in the negative charge contained by pectin. Dissolved pectin is negatively charged at neutral pH and approaches zero charge at low pH. The pKa-value of pectin is about 3.5[22]. The pH of the formulation could therefore affect the degree of ionization of the pectin molecule and its electrostatic interaction with cations. Optimum zeta potential was achieved with 0.5% concentration of pectin and 0.5% of $MgCl_2$.

Results of % drug entrapment efficiency reveals that increase in the concentration of divalent cation does not significantly results in increase in the drug entrapment but increase in pectin concentration significantly results in the increase in the drug entrapment as shown in table 5.2. The increase in % drug entrapment efficiency with increase in pectin concentration is due to porous structure of pectin and more amount of pectin can entrap more amount of drug. The % drug entrapment efficiency was obtained maximum using $MgCl_2$ as a divalent cation as compared to $CaCl_2$ and $ZnCl_2$.

Results of % drug released reveals that increase in the concentration of divalent cation does not significantly make changes in drug release pattern but increase in pectin concentration results significantly in retardation of % drug release due to retardation of drug release with increase in the complex formation. Maximum drug release was obtained with 0.5% concentration of pectin and 0.5% of $MgCl_2$.

Nanoparticulate suspension prepared using $ZnCl_2$ as a divalent cation showed instability within two days so it was not analyzed for invitro drug release study.

B) Effect of pH:[22]

It has been reported that pH of pectin solution have significant effect on particle size of nanoparticles. Therefore, three pH conditions pH 2.0, 4.0 and 6.0 were explored for the preparation of pectin nanoparticles.

Table No 5.6:- Effect of pH on particle size

Divalent cation	pH 2.0	pH 4.0	pH 6.0
$MgCl_2$	920.7 nm	274.6 nm	445.3 nm
$CaCl_2$	876.1 nm	811.4 nm	901.4 nm

$ZnCl_2$	980.2 nm	860.2 nm	942.4 nm

Discussion:

It was observed that in all divalent cations (Mg2+, Ca2+, and Zn2+), the low-pH (4) pectin solution yielded smaller sizes than the high-pH (6). This might be attributable to a higher degree of ionization of the pectin molecule at pH 4, which would allow for greater binding between the negatively charged pectin and the positively charged cations, thereby resulting in smaller size. Dissolved pectin is negatively charged at neutral pH and approaches zero charge at low pH. The pKa-value of pectin is about 3.5. The pH of the formulation could therefore affect the degree of ionization of the pectin molecule and its electrostatic interaction with cations.

On the basis of particle size of pectin nanoparticles at different pH it was found that minimum particle size was obtained at pH 4.0 and using magnesium chloride as a divent cation. Thus 4 pH for pectin solution was used for further preparation of nanoparticles.

Based on the above observations, it is concluded that nanoparticles prepared using $MgCl_2$ as a divalent cation gives smaller particle size, optimum zeta potential and entrapment efficiency and gives almost complete drug release after 24 hours. Thus $MgCl_2$ is used as a divalent cation for further studies.

From the results of preliminary batches, it can be concluded that amongst the various formulation parameters evaluated, pectin:divalent cation concentration ratio and pH of pectin solution, were having significant effect on formulation characteristics of nanoparticles. Hence, taking this in to consideration a 3^2 factorial design was applied in order to identify the factors having significant effect on particle size, zeta potential, % entrapment efficiency and % drug released.

5.1.2 Optimization of the nanoparticles:

In order to obtain best formulation, the relationship between controllable variable and quality variable must be understood. The traditional method used to study this relationship involves "changing one variable at a time, while keeping others as constant". This approach has been proved to be expensive, laborious and also unfavorable to fix errors that are unpredictable and at times even unsuccessful. On the other hand Design of experiment (DoE) can serve as an efficient and economical method of obtaining the necessary information to understand relationship between variables. DoE provides not only efficient use of resources, but also provides a method of obtaining a mathematical model which can be used to characterize and optimize formulation and or process. In a factorial design the influences of all experimental variables, factors, and interaction effects on the response or responses are investigated. If the combinations of k factors are investigated at two levels, a factorial design will consist of 2k experiments.

In preliminary trials it is observed that pectin:cation ratio affects particle size, zeta potential, % entrapment efficiency and % drug released. Furthermore, it is reported that pH of the pectin solution is having significant effect on particlesize.

Thus for the optimization purpose, here 3^2 full factorial design has been used. Pectin : $MgCl_2$ concentration ratio (X_1) and pH of pectin solution (X_2) were selected as independent variables, while particle size, zeta potential, % entrapment efficiency and % drug released were selected as dependent variables.

Table 5.7: Experimental Design, Factors and Responses

Factors (Independent variables)	Design level		Responses (Dependent variables)
	Coded level	Uncoded level	Y_1= Particle size (nm)
X_1: Pectin:$MgCl_2$ ratio	-1	70:30	Y_2= Zeta Potential (mV)
	0	50:50	
	+1	30:70	Y_3= % Drug Entarappment efficiency
X_2: pH of pectin solution	-1	2	
	0	4	
	+1	6	Y_4= % Drug released (24 hrs)

Table 5.8: Composition for experimental formulations

Batch	Variable Factors		Observed Values			
	Pectin:$MgCl_2$	pH of	Particle size (nm)	Zeta Potential	% Drug Entarappment	% Drug released

	ratio (X_1)	pectin solution (X_2)	(Y_1)	(mV) (Y_2)	efficiency (Y_3)	at 24 hours (Y_4)
B1	-1	-1	825.9	-30.9	79.2	70.565
B2	-1	0	241.2	-30.6	78.4	75.452
B3	-1	1	308.8	-29.6	79.4	71.654
B4	0	-1	793.8	-29.4	74.6	85.624
B5	0	0	170.8	-28.9	76.2	90.364
B6	0	1	306.9	-26.4	75.1	86.678
B7	1	-1	1004	-26.1	69.4	79.542
B8	1	0	272	-23.6	70.6	80.264
B9	1	1	428	-22.4	68.5	79.634
CP1	0	-0.5	175.6	-25.5	75.4	92.4
CP2	0	+0.5	180.4	-28.7	74.6	91.6

On the basis of observations from preliminary batches, a 3^2 full factorial design was used for optimization of venlafaxine hydrochloride nanoparticles. The independent variables (factors) were the Pectin:$MgCl_2$ ratio (X_1), and pH of the pectin solution(X_2). The dependent variables (responses) were particle size (nm) (Y_1), zeta Potential (mV) (Y_2), % drug Entarappment efficiency (Y_3) and % drug released at 24 hours (Y_4).

The factors and responses are summarized in table 5.5. Compositions of designed formulations are listed in table 5.7. Statistical model was used to evaluate the response.

Results

		Size (d.nm):	% Intensity	Width (d.nm):
Z-Average (d.nm): 175.6	Peak 1:	185.0	78.6	93.14
PdI: 0.336	Peak 2:	425	6.2	953.5
Intercept: 0.934	Peak 3:	129	3.1	342.2

Result quality : Good

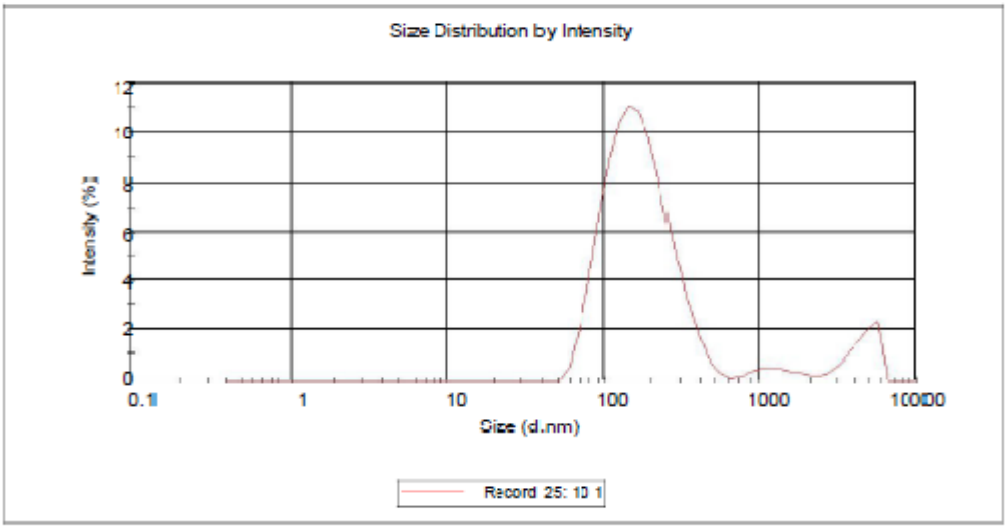

Figure 5.4: Particle size report of batch CP1

Statistical model equation:

To determine the levels of independent variables (factors) that gives optimum Particle size (nm), Zeta Potential (mV), % Drug Entarappment efficiency and % Drug released at 24 hours (Y_4), mathematical relationships were generated between factors and levels. The equations for the responses are given below:

$$Y_1 = 168.344 + 54.683X_1 - 263.333X_2 + 89.483X_1^2 + 383.233X_2^2 - 14.725X_1X_2 \quad (1)$$

$$Y_2 = 75.766 - 4.75X_1 - 0.333X_2 – 1.05X_1^2 - 0.70X_2^2 - 0.275X_1X_2 \quad (2)$$

$$Y_3 = 75.744 + 4.783X_1 + 2.33X_2 - 1.016X_1^2 - 0.66X_22 - 0.325X_1X_2 \quad (3)$$

$$Y_4 = 89.616 + 3.613X_1 + 0.387X_2 – 11.385X_1^2 – 3.092X_2^2 – 0.226X_1X_2 \quad (4)$$

Table 5.9: Observed and Predicted Values of Y_1, Y_2, Y_3 and Y_4

Batch	Y_1 (nm)	Y_2 (mV)	Y_3 (%)	Y_4 (%)

	Observed	Predicted	Observed	Predicted	Observed	Predicted	Observed	Predicted
B1	825.9	889.668	-30.9	-31.89	79.2	80.3	70.565	70.913
B2	241.2	270.345	-30.6	-31.55	78.4	79.5	75.452	74.618
B3	308.8	337.769	-29.6	-28.64	79.4	79.8	71.654	72.139
B4	793.8	760.227	-29.4	-27.52	74.6	75.5	85.624	86.137
B5	170.8	113.660	-28.9	-26.75	76.2	77.8	90.364	89.616
B6	306.9	288.244	-26.4	-26.42	75.1	75.6	86.678	86.911
B7	1004	919.118	-26.1	-26.18	79.4	80.5	79.452	78.591
B8	272	275.827	-23.6	-24.78	70.6	71.8	80.264	81.844
B9	428	417.685	-22.4	-22.03	68.5	69.7	79.634	78.913
CP1	175.6	155.7	-27.5	-25.8	75.4	76.5	92.400	91.248
CP2	180.4	158.3	-28.7	-26.82	74.6	75.1	91.601	90.246

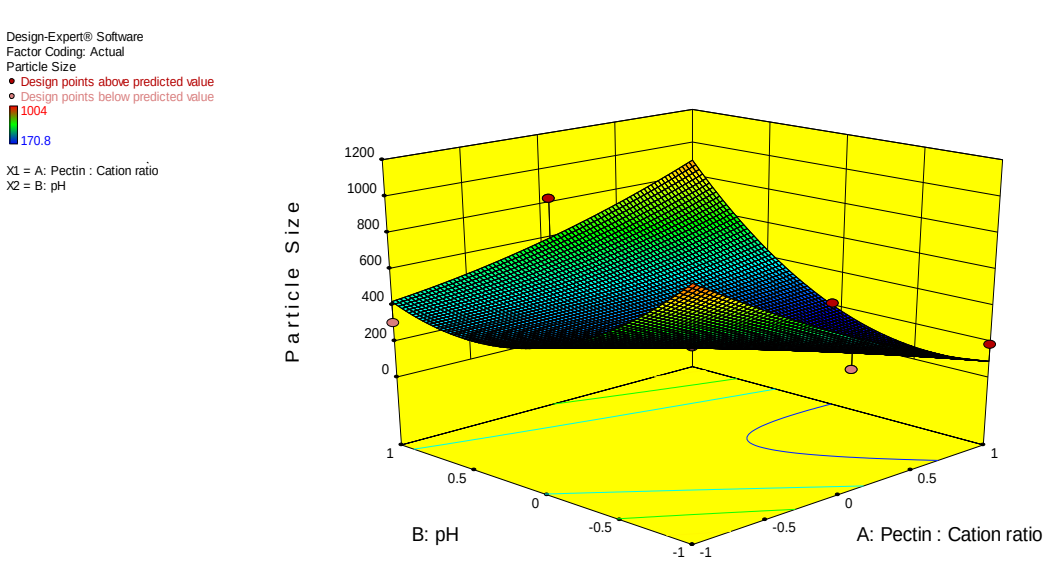

Figure 5.5: Surface plot of particle size

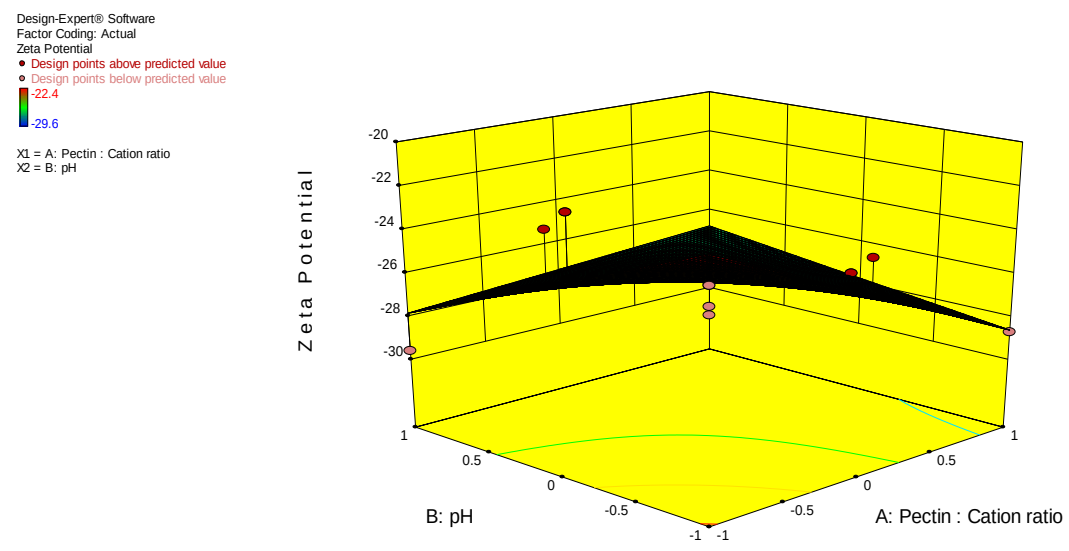

Figure 5.6: Surface plot of zeta potential

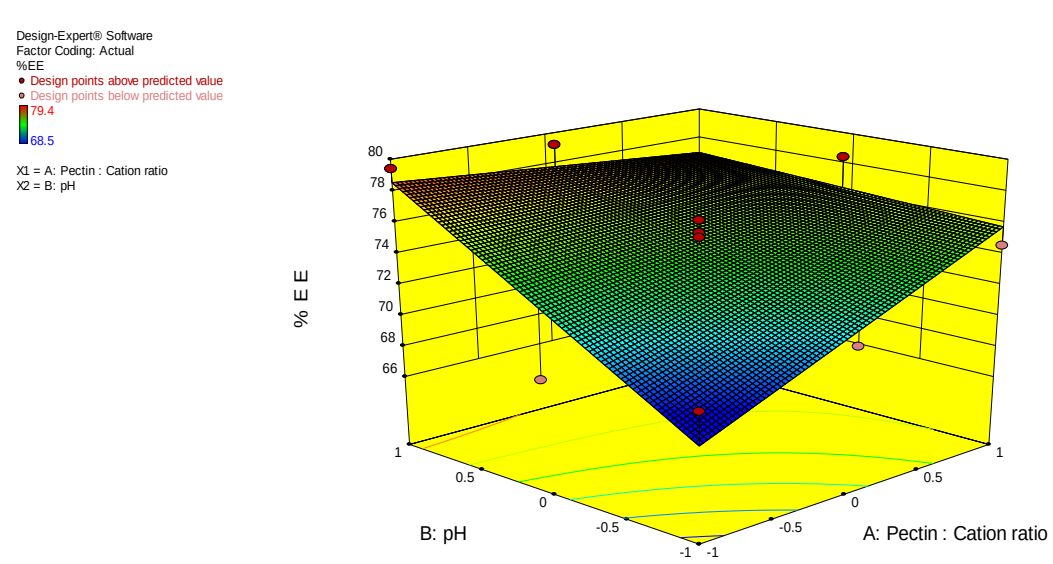

Figure 5.7: Surface plot of % Drug entrappment efficiency

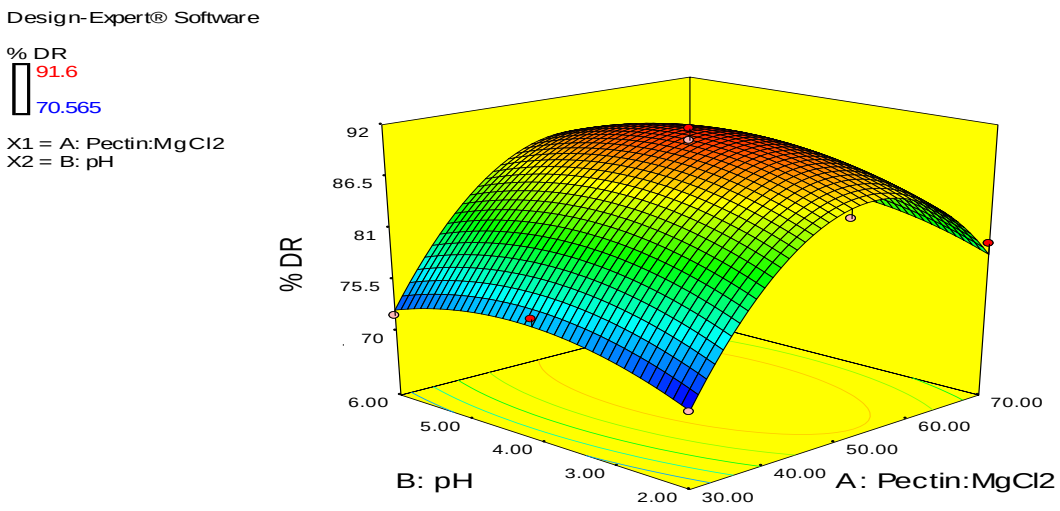

Figure 5.8: Surface plot of % Drug entrappment efficiency

Equation 1 shows relation between particle size and independent variable. It was observed that X_1 is directly proportional and X_2 is inversely proportional to particle size. As the amount of pectin and $MgCl_2$ increases, particle size increases.

Further equation 2 shows relation between zeta potential and independent variables. It was observed that X_1 and X_2 had inverse effect on zeta potential. As the amount of pectin and $MgCl_2(X_1)$ increases, zeta potential decreases.

Further equation 3 shows relation between % Drug Entrappment efficiency and independent variables. It was observed that X_1 and X_2 had positive effect on zeta potential. As the amount of pectin and $MgCl_2$ increases, % Drug Entrappment efficiency increases.

Further equation 4 shows relation between % Drug released at 24 hours and independent variables. It was observed that X_1 and X_2 had direct effect on % Drug released at 24 hours. As the amount of pectin and $MgCl_2$ increases, % Drug released at 24 hours decreases.

Response surface and overlay plot for all responses were established. In order to check validity of study, two new batches with predicted values of responses were prepared. The predicted and observed values of both responses are shown in table 5.9, which indicates good conformity. Thus it can be said that generated model can be used to predict responses within the factorial design space.

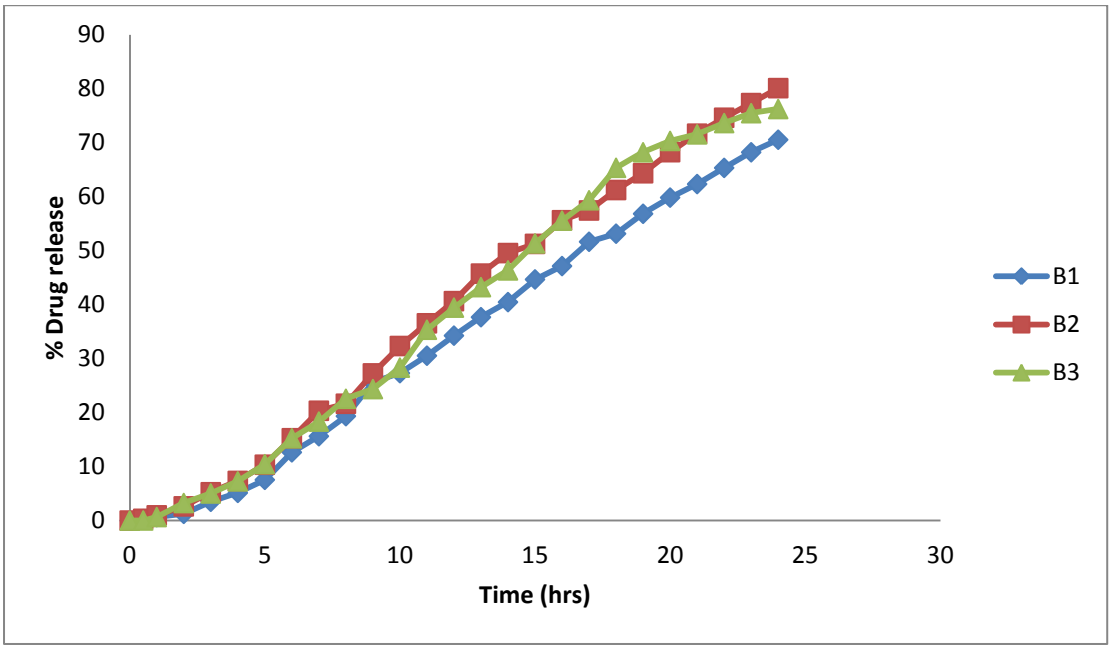

Figure 5.9: % Drug release profile for batches B1 to B3

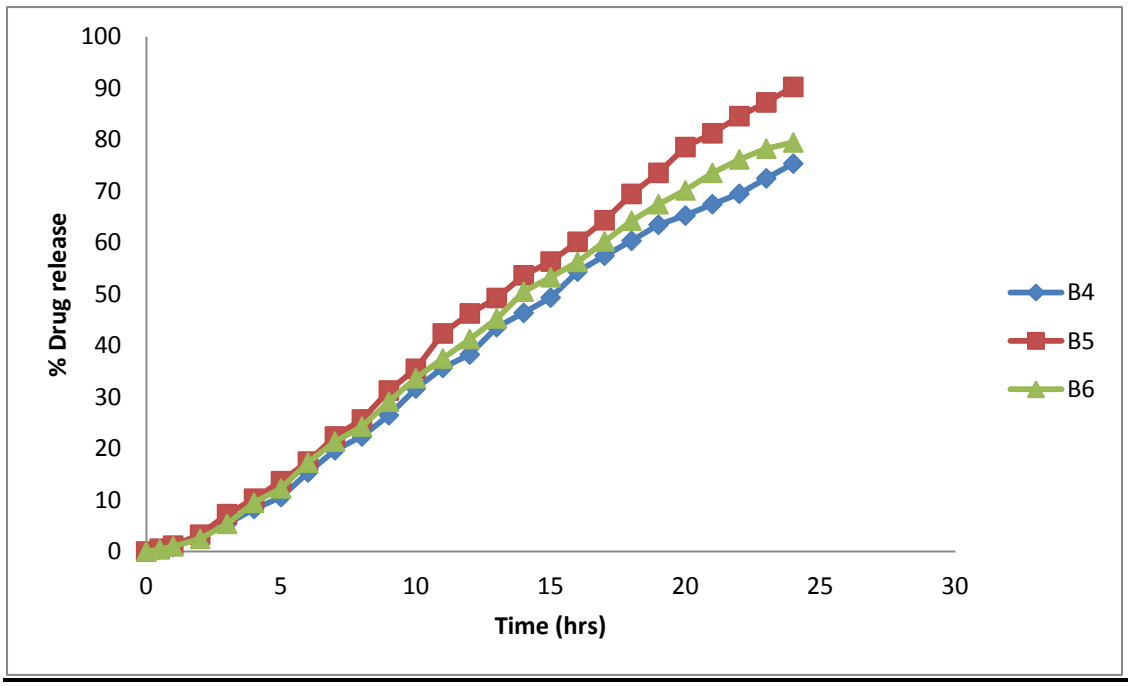

Figure 5.10: % Drug release profile for batches B4 to B6

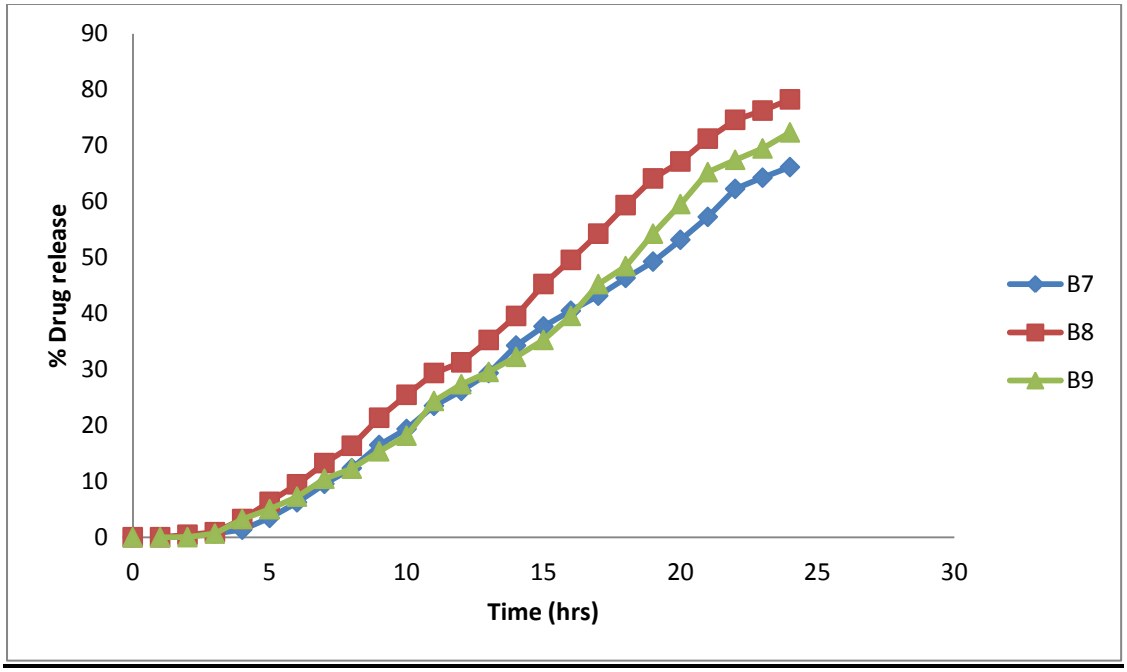

Figure 5.11: % Drug release profile for batches B7 to B9

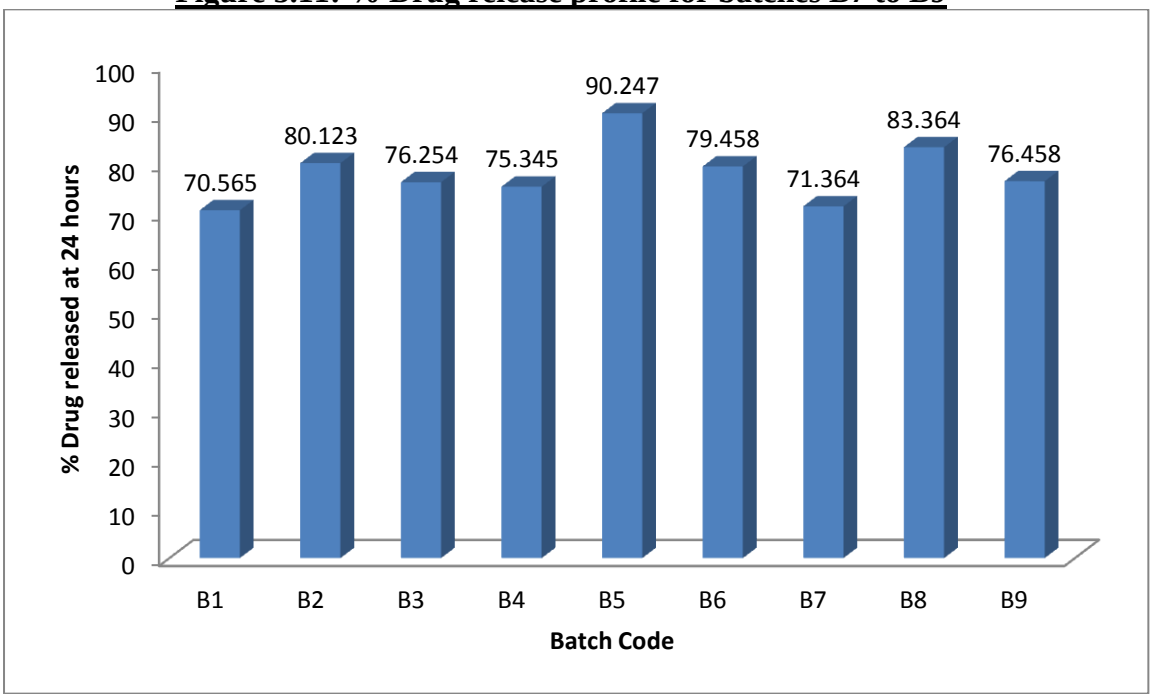

Figure 5.12: % Drug release after 24 hours for batches B1 to B11

Conclusion: From the results of particle size, zeta potential, % drug entrapment efficiency and cumulative % drug released it is concluded that batches B5 (0.5 % pectin and 0.5% $MgCl_2$) gives lowest particle size,optimum zeta potential, % drug entrapment efficiency and cumulative % drug release was almost 100% after 24 hours. So 0.5 % pectin and 0.5% $MgCl_2$ was selected as optimized formula.

5.1.3 Optimization of insitu gelling solution:[25,26,28]

From the preliminary batches using different concentrations of Poloxamer 407, HPMC K4M effects insitu gelling time and temperature. Results of various batches prepared using different concentrations of poloxamer 407 and HPMC K4M are shown in table 5.10.

Table 5.10: Results of different batches prepared for insitu gelling solution

Batch No	Concentration of Poloxamer 407	Concentration of HPMC k4M	Insitu gelling temperature(^{O}C)	Insitu gelling time (Minutes)
P1	15	0.1	38	8
P2	15	0.3	36	5
P3	15	0.5	34	4.5
P4	15	0.7	34	3
P5	20	0.5	34	3
P6	25	0.5	31	< 40 sec
P7	30	0.5	30	< 40 sec

Determination of insitu gelling temperature: [28]

In situ gelling temperature is determined using Brookfield viscometer. Solution is heated slowly at 1^{0}C till the gel is obtained and is observed by increase in the viscosity.

Discussion: Different batches for the optimization of insitu gelling polymeric phase were prepared as shown in table 5.8. Initially concentration of poloxamer 407 was kept fixed (15%) and concentration of HPMC K4M was increased from 0.1-0.7 %. But optimum insitu gelling temperature and insitu gelling time was not achieved.

So for further optimization concentration of poloxamer 407 was raised from 15% to 30% and concentration of HPMC K4M was kept constant at 0.5% as shown in table 5.8.

From the results of this preliminary batches for the optimization of polymeric phase it was concluded that optimum insitu gelling temperature and insitu gelling time was achieved with 25% poloxamer 407 and 0.5% HPMC K4M.

Conclusion: From the result of above batches it is observed that optimum insitu gelling temperature and gelling time is achieved with 25% poloxamer 407 and 0.5% HPMC K4M.

To the prepated nanoparticulate suspension 25% poloxamer 407 and 0.5% HPMC K4M was added for further studies.To this 1% stearic acid was added as a stabilizer.

Invitro Diffusion study:[28]

To the nanoparticulate suspension of batches B5, Poloxamer 407 (25%), HPMC K4M (5%), carbopol 934P (2%), stearic acid (1%) were added and evaluated for invitro diffusion using Franz diffusion cell. Isolated rat nasal mucosa was used as a semipermeable membrane. The test product was applied to the membrane via the top chamber. The bottom chamber was filled with 25 ml of simulated nasal electrolyte solution (7.45 mg/ml NaCl, 1.29 mg/ml KCl, and 0.32 mg/ml $CaCl_2 \cdot 2H_2O$ and pH adjusted at 5.5) used as a dissolution medium at 37±0.5°C from which samples were taken at regular intervals for analysis. The amount of drug released from the formulation was measured spectrophotometrically at λmax 226 nm. The concentration of drug was determined from a previously constructed calibration curve.

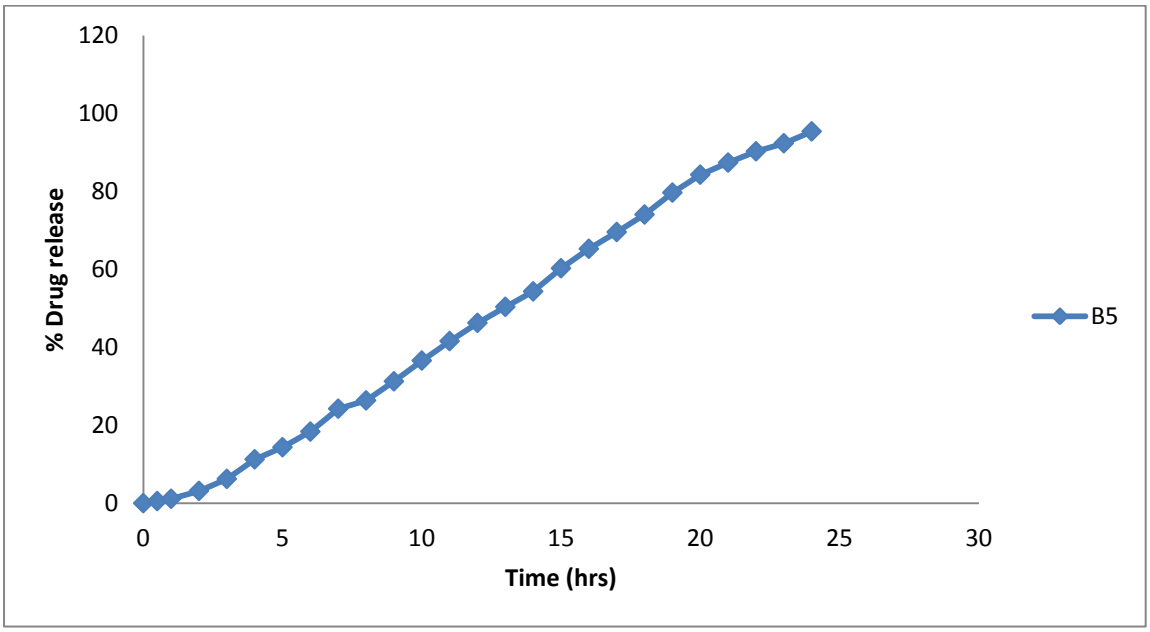

Figure 5.13:- % Drug release profile for batch B5

Mucoadhesive strength:[31]

Mucoadhesive strengths of the gels were determined by measuring the force required to detach nasal mucous membrane from the gel using texture analyser. Freshly excised goat nasal membrane was attached to the upper probe of the instrument, and the fixed amount of gel was kept below that. The upper probe was then lowered at a speed of 10 mm/min to touch the surface of the gel. A force of 0.1 Newton was applied for 5 min to ensure intimate contact between the membrane and the gel. The surface area of exposed mucous membrane was 1.13 cm^2.

Table 5.11: Results of mucoadhesive strength for batches B5

Batch No	Mucoadhesive strength
B5	17.25 gm

Conclusion:

From the results of particle size, zeta potential, % drug incorporation efficiency, % drug released of various batches prepared using factorial design it was concluded that insitu gelling nanoparticulate nanosuspension prepared using 0.5% pectin at pH 4 and 0.5% $MgCl_2$ gives minimum particle size, optimum zeta potential, optimum drug incorporation, optimum mucoadhesion and complete drug release after 24 hours.

Ionotropic gelation technique was used for the preparation of pectin nanoparticles in the present study in which pectin was used as a polymer and $MgCl_2$, $CaCl_2$ and $ZnCl_2$ were used as a divalent cation.

In the preliminary trials nanoparticles were prepared using pectin in the concentration range of 0.5-1.0% and different divalent caations in the concentration range of 0.5-1.0%. Different batches using pectin in concentration of 0.5% and 1% with $MgCl_2$, $CaCl_2$ and $ZnCl_2$ in concentration range of 0.5% and 1% were prepared and analysed for particle size, zeta potential, % drug entrapment efficiency and % drug released.

Results of particle size reveals that increase in the concentration of divalent cation does not significantly results in increase in the particle size but increase in pectin concentration significantly results in the increase in the particle size. The increase in particle size with increase in pectin concentration is due to increase in globule size with increase in polymer concentration. Nanoparticles prepared using Mg^{+2} were smaller in size than Ca^{+2} and Zn^{+2} (when formulated using the same amount and ratio of pectin/ divalent cations). Minimum particle size was achieved with 0.5% concentration of pectin and 0.5% of $MgCl_2$.

Results of zeta potential reveals that increase in the concentration of pectin and divalent cation results in increase in the negative zeta potential. The increase in zeta potential with increase in pectin and is due to increase in the negative charge contained by pectin. Dissolved pectin is negatively charged at neutral pH and approaches zero charge at low pH. The pKa-value of pectin is about 3.5. The pH of the formulation could therefore affect the degree of ionization of the pectin molecule and its electrostatic interaction with cations. Optimum zeta potential was achieved with 0.5% concentration of pectin and 0.5% of $MgCl_2$.

Results of % drug entrapment efficiency reveals that increase in the concentration of divalent cation does not significantly results in increase in the drug entrapment but increase in pectin concentration significantly results in the increase in the drug entrapment. The increase in % drug entrapment efficiency with increase in pectin concentration is due to porous structure of pectin and more amount of pectin can entrap more amount of drug. The % drug entrapment efficiency was obtained maximum using $MgCl_2$ as a divalent cation as compared to $CaCl_2$ and $ZnCl_2$.

Results of % drug released reveals that increase in the concentration of divalent cation does not significantly make changes in drug release pattern but increase in pectin

concentration results significantly in retardation of % drug release due to retardation of drug release with increase in the complex formation. Maximum drug release was obtained with 0.5% concentration of pectin and 0.5% of $MgCl_2$.

It has been reported that pH of pectin solution have significant effect on particle size of nanoparticles. Therefore, three pH conditions pH 2.0, 4.0 and 6.0 were explored for the preparation of pectin nanoparticles and it was observed that in all divalent cations (Mg^{2+}, Ca^{2+}, and Zn^{2+}), the low-pH 4 pectin solution yielded smaller sizes than the high-pH 6. This might be attributable to a higher degree of ionization of the pectin molecule at pH 4, which would allow for greater binding between the negatively charged pectin and the positively charged cations, thereby resulting in smaller size. Dissolved pectin is negatively charged at neutral pH and approaches zero charge at low pH. The pKa-value of pectin is about 3.5. The pH of the formulation could therefore affect the degree of ionization of the pectin molecule and its electrostatic interaction with cations. Lowest particle size was obtained with 0.5% pectin and 0.5% $MgCl_2$ at pH 4.0 (i.e. 274.6 nm).

For the systematic optimization of the prepared nanoparticles a 3^2 full factorial design was used with Pectin:$MgCl_2$ concentration ratio and pH of the pectin solution as independent variables and particle size, zeta potential, % entrapment efficiency and % drug release at 24 hours as dependent variables. Results of different batches prepared using factorial design revealed that nanoparticles prepared using 0.5% pectin solution, 0.5 % $MgCl_2$ and pH 4.0 of pectin solution had lowest particle size (170.8 nm), optimum zeta potential (-28.9 mV), optimum % entrapment efficiency (76.2%) and complete drug release at 24 hours (90.36%).

Results of preliminary batches prepared for the optimization of insitu gelling polymeric phase revealed that formula containing 25% poloxamer 407 and 0.5% HPMC K4M had optimum insitu gelling temperature (31^oC) and insitu gelling time (< 40 seconds).

The prepared nanoparticles were incorporated into optimized thermosensitive insitu gelling solution and further evaluated for invitro diffusion study. Results revealed almost complete drug release (95.354 %) from the gel that is of great importance in case of antidepressive therapy.

From this study it can be concluded that nanoparticulate insitu gelling system can be used for nasal administration of venlafaxine hydrochloride to enhance the CNS targetting, bioavailability and patient compliance.

References

1. Alam M., Beg S., Samad A., Baboota S., Kohla K., Ali J., Ahuja A., Akbar M., Strategy for effective brain drug delivery. European Journal of Pharmaceutical Sciences, 40, 2010, 385–403.

2. Lochhead J., Thorne R. Intranasal delivery of biologics to the central nervous system, Advanced Drug Delivery Reviews, 2012, 614–628.

3. Hussain A. Intranasal drug delivery, Advanced Drug Delivery Reviews 29, 1998, 39–49.

4. Illuma L. Nasal drug delivery-possibilities, problems and solutions. Journal of Controlled Release 87, 2003 187–198.

5. Martindale the complete drug reference, Pharmaceutical press USA, 36th edition Volume I; 2009, Page No 845.

6. Indian Pharmacopies. Government of India Ministry of Health and Family Welfare. Published by The Indian Pharmacopoiea Commission. Ghaziabad, 2010, Volume II: 825, 1256.

7. British pharmacopoeia, 2010, Volume II, 2341.

8. United Staates Pharmacopoiea, 2010, Volume II, 2214

9. Acharya D., Design and Development of Modified release venlafaxine hydrochloride capsule, International Journal of Pharmacy and Pharmaceutical Sciences, 2013, 78-83.

10. Anton N., Formulation and Development of Venlafaxine Hydrochloride capsules, International Journal of Pharmaceutics 452, 2012, 89-95.

11. Sriamornsak P. Chemistry of Pectin and Its Pharmaceutical Uses : A Review, 206-228..

12. Thorat R., Patil P., Aage R., Puranik P., Salve V. Formulation Development and Evaluation of Venlafaxine HCl sustained release matrix tablet. International Journal of Pharmacy and Pharmaceutical Sciences, 2013, 757-765.

13. Pund S., Rasve G., Borade G. Ex vivo permeation characteristics of venlafaxine through sheep nasal mucosa. European Journal of Pharmaceutical Sciences 48, 2013, 195–201.

14. Wang X,, Chi N., Tang X. Preparation of estradiol chitosan nanoparticles for improving nasal absorption and brain targeting. European Journal of Pharmaceutics and Biopharmaceutics 70, 2008, 735–740.

15. Beduneau A., Hindre F., Clavreul A., Leroux J., Saulnier P., Benoit J. Brain targeting using novel lipid nanovectors, Journal of Controlled Release 126, 2008, 44–49.

16. Luppi B., Bigucci F., Abruzzo A. , Corace G., Cerchiara T., Zecchi V. Freeze-dried chitosan/pectin nasal inserts for antipsychotic drug delivery, European Journal of Pharmaceutics and Biopharmaceutics 75, 2010, 381–387.

17. Abdelbary A., Tadros M. Brain targeting of olanzapine via intranasal delivery of core-shell difunctional block copolymer mixed nanomicellar carriers: In vitro characterization, ex vivo estimation of nasal toxicity and in vivo biodistribution studies, International Journal of Pharmaceutics 452, 2013, 300–310.

18. Chertok B., Bradfrd B., David A., Yu F., Bergemann C., Ross B., Yang V. Iron oxide nanoparticles as a drug delivery vehicle for MRI monitored magnetic targeting of brain tumors Biomaterials 29, 2008, 487–496.

19. Gao X., Chen J., Tao W., Zhu J., Zhang Q., Chen H., Jiang X. UEA I-bearing nanoparticles for brain delivery following intranasal administration, International Journal of Pharmaceutics 340, 2007, 207–215.

20. Wen Z., Yan Z., Hu K., Pang Z., Cheng X., Guo L., Zhang Q., Jiang X., Fang L. Odorranalectin-conjugated nanoparticles: Preparation, brain delivery and pharmacodynamic study on Parkinson's disease following intranasal administration, Journal of Controlled Release 151, 2011, 131–138.

21. Opanasopit P., Apirakaramwong A., Ngawhirunpat T, Rojanarata T., Ruktanonchai U. Development and Characterization of Pectinate Micro/Nanoparticles for Gene deliveri. AAPS PharmSciTech,Volume 9, No 1, March 2008, 67-74.

22. Nagavarma BVN, Hemant K Yadav, Ayaz Vasudha, Shivakumar H, Different techniques for preparation of polymeric nanoparticles- a review, Asian journal of pharmaceutical and clinical research, Vol 5, Suppl 3, 2012, 16-23

23. Vyas T., Babbar A., Sharma R., Singh S., Misra A. Preliminary Brain-targeting Studies on Intranasal Mucoadhesive Microemulsions of Sumatriptan, AAPS PharmSciTech 2006, 1-9.

24. Qian S.,Wong C., Zuo Z. Development, characterization and application of in situ gel systems for intranasal delivery of tacrine. International Journal of Pharmaceutics 468, 2014, 272-282.

25. Patel A., Gondkar S., Saudagar R. Design and evaluation of mucoadhesive gel of glimipride for nasal delivery. American journal of pharmacy and healthcare, 2013, 2231-3647.

26. Ved P., Kim K., Poly(ethylene oxide/propylene oxide) copolymer thermo-reversible gelling system for the enhancement of intranasal zidovudine delivery to the brain. International Journal of Pharmaceutics 411, 2011, 1–9.

27. Saindane N., Pagar K, Vavia P. Nanosuspension based insitu gelling nasal spray of carvedilol:Development, invitro and invivo characterization.AAPS PharmSciTech, 2013, 189-199.

28. Haque S., Shadab M, Fazil M., Kumar M., Kaur J., Ali J, Baboota S.Venlafaxine loaded chitosan nanoparticles for brain targeting, Pharmacoinetic and Pharmacodynamic evaluation. Carbohydrate Polymers 89, 2012,72-79.

29. Patil P., Chavanke D., Wagh M. A review on ionotropic gelation method: Novel approach for controlled gastroretentive gelispheres. International Journal of Pharmacy and Pharmaceutical Sciences, vol 4, 27-32.

30. Basu S., Kumar A., Bandyopadhyay. Characterization of mucoadhesive nasal gels containing midazolam hydrochloride prepared from Linum usitatissimum L. mucilage, Brazilian Journal of Pharmaceutical Sciences, vol. 47, 2011, 817-823.

31. Zaki N., Awad G., Mortada N. Enhanced bioavailability of metoclopramide HCl by intranasal administration of a mucoadhesive in situ gel with modulated rheological and mucociliary transport properties. European journal of Pharmaceutical sciences 32, 2007, 296-307.

32. Majithiya R., Ghosh P., Umrethia M., Murthy R.Thermoreversible mucoadhesive gel for nasal delivery of Sumatriptan, AAPS PharmSciTech, 2006, 104-111.

33. Gowda D, Khan M.Formulation and evaluation of in situ gel of diltiazem hydrochoride for nasal delivery. Der Pharmacia Lette, 2011, 371-381.

34. Kumar J., Muralidharan S,, Arumugam S. A review on polymeric in-situ gel system. Journal of Pharmacy and Pharmaceutical sciences, 2013, 89-95.

35. Serralheiro A., Alves G., Fortuna F., Falcao A. Intranasal administration of carbamazepine to mice: A direct delivery pathway for brain targeting. European journal of pharmaceutical sciences 60, 2014, 32-39.

36. Kumar K., Kakkar V., Mishra A., Chuttani K., Kaur I. Intranasal delivery of streptomycin sulfate loaded solid lipid nanoparticles to brain and blood. International journal of pharmaceutics 461, 2014, 223-233.

37. Dufes C., Olivier J., Gaillard A., Couet W. Brain delivery of vasoactive intestinal peptide following nasal administration to rats. International journal of pharmaceutics 255, 2003, 87-97.

38. Seju U., kumar K., Sawant A. Development and evaluation of olanzapine loaded PLGA nanoparticles for nose to brain delivery: Invitro and Invivo studies. Acta Biomaterialia 7, 2011, 4169-4176.

39. Makhija S., Vavia P. Once daily sustained release tablets of venlafaxine, a novel antidepressant. European journal of pharmaceutics and biopharmaceutics, 2002, 174-182.

40. Charlton S., Davis S., Illum L. Evaluation of bioadhesive polymers as delivery systems for nose to brain delivery: In vitro characterisation studies. Journal of Controlled Release 118, 2007, 225–234.

41. Beduneau A., Saulnier P., Benoit J. Active targeting of brain tumors using nanocarriers, Biomaterials 28, 2007, 4947–4967.

42. Nagpal K., Singh S. and Mishra D. Chitosan Nanoparticles: A Promising System in Novel Drug Delivery, Chem. Pharm. Bull, 58, 1423—1430.

43. Li L., Nandi N., Kim K. Development of an ethyl laurate-based microemulsion for rapid-onset intranasal delivery of diazepam. International Journal of Pharmaceutics, 2002, 77–85.

44. Zhang Q., Jiang X., Jiang W., Su L., Shi Z. Preparation of nimodipine-loaded microemulsion for intranasal delivery and evaluation on the targeting efficiency to the brain International Journal of Pharmaceutics 275, 2004, 85–96.

45. Pal S., Jana U., Manna P., Mohanta G., Manavalan R. Nanoparticle: An overview of preparation and Characterization Journal of Applied Pharmaceutical Science 01, 2011, 228-234.

46. Ugwoke M., Agu R., Verbeke N., Kinget R. Nasal mucoadhesive drug delivery: Background, applications, trends and future perspectives. Advanced Drug Delivery Reviews 57, 2005, 1640– 1665.